International Journal of Forecasting 34 (2018) 314–335

Contents lists available at ScienceDirect

International Journal of Forecasting

journal homepage: www.elsevier.com/locate/ijforecast

Data-based mechanistic modelling and forecasting globally averaged surface temperature

Peter C. Young *

Lancaster Environment Centre, Lancaster University, UK
Integrated Catchment Assessment and Management Centre, Australian National University College of Medicine, Biology & Environment Canberra, ACT, Australia

ARTICLE INFO

Keywords:
Global Temperature Anomaly
Data-Based mechanistic modelling
Differential equation model
Quasi-cyclic variations
Adaptive forecasting

ABSTRACT

The main objective of this paper it to model the dynamic relationship between global averaged measures of *Total Radiative Forcing* (RTF) and surface temperature, measured by the *Global Temperature Anomaly* (GTA), and then use this model to forecast the GTA. The analysis utilizes the *Data-Based Mechanistic* (DBM) approach to the modelling and forecasting where, in this application, the unobserved component model includes a novel hybrid Box-Jenkins stochastic model in which the relationship between RTF and GTA is based on a continuous time transfer function (differential equation) model. This model then provides the basis for short term, inter-annual to decadal, forecasting of the GTA, using a transfer function form of the Kalman Filter, which produces a good prediction of the 'pause' or 'levelling' in the temperature rise over the period 2000 to 2011. This derives in part from the effects of a quasi-periodic component that is modelled and forecast by a *Dynamic Harmonic Regression* (DHR) relationship and is shown to be correlated with the *Atlantic Multidecadal Oscillation* (AMO) index.

1. Introduction

Most climatic modelling research conforms to the 'scientific method', following what Popper (1959) has termed a 'hypothetico-deductive' approach. But Popper's philosophical stance is based mainly on his consideration of laboratory-based science: one has only to search for the word 'experiment' in his famous book to realise how important experimentation, and particularly planned experimentation, is in his view of the scientific method. Such planned experimentation can help, of course, to minimize noise and remove any ambiguity on measured data, so clarifying understanding of the potentially complex mechanisms that underlie this observed behaviour. Unfortunately, it is not possible to conduct well planned experiments on large, naturally occurring systems, such as the global climate, and so modelling has to be based on data collected during the 'normal operation' of the system.

This hypothetico-deductive approach to scientific research can be contrasted with the *inductive* method, which has a rich history in science (Young, 2012). Induction is the opposite of deduction: it starts by taking as many observations of the natural system as possible, with the aim of inferring from these data alone how the system works, without the introduction of any hypotheses that may be prejudicial and so distort the modelling process. In the real world, of course, this differentiation between these two approaches to scientific research is too simplistic: inductive and hypothetico–deductive modelling are synergistic activities, the relative contributions of which will depend upon the system being modelled and the information of *all* types, not only time-series data, that are available.

* Correspondence to: Lancaster Environment Centre, Lancaster University, UK.
E-mail address: p.young@lancaster.ac.uk.

https://doi.org/10.1016/j.ijforecast.2017.10.002

The present paper applies the *Data-Based Mechanistic* (DBM) method of modelling, forecasting and control (see chapter 12 in Young, 2011 and the prior references therein) to globally averaged surface temperature data, as represented here and most other publications on this topic by the Global Temperature Anomaly (GTA) series (see later, Section 5). This approach is primarily based on induction but it attempts to produce models that can be interpreted in an understandable mechanistic manner; i.e. in manner which relates to the mechanisms that are normally used to describe the nature of the system being analysed, as well as the concepts and assumptions that underlie the way these mechanisms are described in mathematical terms. This DBM model normally relates input signals of some kind to the outputs that are most likely to be influenced by these inputs.

Climate modellers tend to use a standard hypothetico-deductive approach but the nature of the system does not allow them to exploit planned experimentation. This often results in complex, high order models based on deterministic, ordinary or partial differential equations. As a result of the high order and the associated large number of model parameters, standard optimization based on simple cost functions is not possible and resort needs to be made to other procedures. An interesting discussion on the difficulties of optimizing these models and some ways of handling these difficulties is given in Neelin, Bracco, Luo, McWilliams, and Meyerson (2010). They point out that the underlying nature of the system has an enormous impact on which of the strategies that are available for the evaluation of sensitivity and optimization are most suitable. The model parameters and the associated range of possible values are normally chosen on a scientific basis based on their physical interpretation and function within the model. Model evaluation normally involves a critical examination of the simulated behaviour in response to internal or external inputs. Sometimes this is accompanied by the application of parametric sensitivity analysis, which indicates which parameters are most affecting the simulated response and so are deserving of particular attention and optimization.

The main inputs that are thought to most affect the GTA are the various globally averaged 'radiative forcing' signals, of which the best known is the greenhouse gas, atmospheric carbon dioxide. It is appropriate, therefore, that DBM models of global surface temperature behaviour, based on the available globally averaged radiative forcing and surface temperature data, should be formulated in terms of similar differential equation models to those used in simpler global climate 'emulation' models (see later Section 3). In contrast to most climate models, however, the DBM models considered in the present paper are inherently stochastic and of a normally low dynamic order that reflects the few 'modes' of dynamic behaviour that, as we shall see, dominate both the simulated output of the large climatic models and the real globally averaged data.

This DBM approach to modelling and forecasting can be contrasted also with the methodology used most often by the forecasting profession, where the standard inductive approach is usually based on discrete-time, 'black box' statistical models with various degrees of complexity. Continuous-time models are used in some applications, such as stock prices, but these are normally in the form of purely stochastic differential diffusion equations based on the application of complex Itô calculus, rather than, as here, ordinary differential equations represented by simple transfer functions in the differential operator.

It is not clear why there has been a reticence to use such continuous-time transfer function models for forecasting but it may be that the methods of statistical identification and estimation for such models are not well known because they were developed originally within the control and systems community (see chapter 8 in Young, 2011 and the prior references therein, going back to the first optimal solution proposed in 1980 Young and Jakeman, 1979). However, there are number of reasons why it can be advantageous to use continuous-time models (Garnier & Young, 2014), in addition to the obvious advantage that such models are better suited for the analysis of rapidly sampled time series, where discrete-time models can encounter estimation difficulties if the eigenvalues of the model are too close to the unit circle in the complex domain. It is felt, therefore, that the forecasting community might consider continuous-time models when the system being modelled is affected dynamically by inputs entering through transfer function models and/or the system description needs to be interpreted in a mechanistic manner. In simple terms, this means that the equivalent and familiar discrete-time equation containing lagged outputs (dependent or target variables) and inputs (independent, explanatory or exogenous variables) is replaced by a related differential equation, with the discrete-time lag operators replaced by suitable differential operators (see Section 4.1).

Bearing in mind the above remarks, the main objective of the present paper is to synthesize a continuous time, differential equation model, considered in a convenient transfer function form, for the changes in globally averaged surface temperature arising from the measured changes in total radiative forcing. In particular, this model needs to be well suited for relatively short term, inter-annual to decadal, prediction of the temperature where, as pointed out by an anonymous reviewer, techniques employing explicit time-stepped numerical simulation models currently run into difficulties caused by 'initialization and cold-start' problems (see e.g. http://blogs.nature.com/climatefeedback/2007/06/predictions_of_climate.html; and Meehl et al., 2007). As such, this differential equation model needs to represent efficiently the dominant modal behaviour of the global climate system; and it should be a stochastic model, obtained using optimal methods of statistical inference, so that it can quantify the uncertainty in the predictions over the forecasting interval.

Finally, note that this kind of stochastic-dynamic modelling is as important as the forecasting in the present study. Indeed, if forecasting alone was the objective, then a simpler approach based, for example, on univariate time series modelling and forecasting, can provide somewhat inferior but still acceptable short-term forecasts of the GTA, as shown in Section 6.3.2 of the paper. But such a univariate approach is purely black box in form and so does not conform with the aims and philosophy of DBM approach to modelling and forecasting.

2. Modelling globally averaged surface temperature

The large and complex global climate models have an important role to play in studying the detailed nature of climate change. However, as Shackley, Young, Parkinson, and Wynne (1998) have suggested, they are not the only, nor necessarily the best models for supporting other tasks associated with the climate *at the global scale*, such as forecasting globally averaged temperature variations. There is an extensive literature on global climate modelling and the recent paper by Fildes and Kourentzes (2011) provides an excellent review of this literature within a forecasting context.

More specifically, the present paper will confirm previous research by the author and others (see e.g. Geoffroy et al., 2013; Jarvis and Li, 2011; Li and Jarvis, 2009; Li, Jarvis, and Leedal, 2009; Young and Parkinson, 2002; Young, Parkinson, and Lees, 1996; Young and Ratto, 2011, as well as other references cited therein) which has shown that normally, despite their complexity, the globally averaged response characteristics of these large models, as well as other, simpler but still quite high order 'emulation' models (see later Section 3), are defined almost completely by a relatively small number of 'dominant dynamic modes' (Young, 1999). And it is these dominant modes of behaviour that are most important in applications such as short to medium term forecasting and the management of carbon emissions (see e.g. Young, 2006; Jarvis, Leedal, Taylor, & Young, 2009; Jarvis, Young, Leedal, & Chotai, 2008; Young & Jarvis, 2002; [1]).

Standard time series models and forecasting methods have been used in previous research on the *Global Temperature Anomaly* (GTA), which is the time series of the changes in the globally averaged mean temperature about a reference level based an average global mean temperature level over a prescribed period (in the present paper between 1951 and 1980). Mills (2010) points to the long history of meteorological time series being analysed by statisticians and cites a number of references in this regard. His own 'structural' model analysis of the GTA does not include an input variable, although he does consider a radiative forcing input in one paper (Mills, 2009) but within an alternative cointegration setting based on the prior analysis of Kaufmann, Kauppi, and Stock (2006a, b), as well as Stern and Kaufmann (2014). Fildes and Kourentzes (2011) consider the validation and forecasting accuracy of GTA models. In their own study, they use CO_2 emissions as an 'explanatory variable' in their multivariate *Neural Network* (NN) model but the dynamic mechanism relating this to the GTA is hidden within the NN.

The most obvious difference between these previous studies and the present paper is that they are concerned mainly with the identification and use of 'black-box', discrete-time difference equations, such as unobserved component and structural models, that derive from the more traditional approaches to time-series analysis and forecasting (Box, Jenkins, and Reinsel, 1994; Harvey, 1989). A quite different *deterministic* time series approach that has appeared in the climatic literature is that of van Hateren (2013). Although he suggests that this is based on 'fractal analysis and e-folding', this is deceptive because the model is simply the sum of first-order low-pass filters with different time constants. While this can be related loosely to some aspects of the DBM model considered in the present paper, the overall approach to model identification and optimization is rather subjective and largely deterministic.

Although DBM models are developed initially in a black-box transfer function form and utilize methods of statistical inference that are related to the structural models mentioned above, the main dynamic relationship that links the sum of all the radiative forcing inputs, or *Total Radiative Forcing* (TRF), to the GTA is identified by a *continuous-time differential* equation, as represented by its equivalent continuous-time transfer function. This is of the same general differential equation form as those used in the construction of global climate models; and they define immediately parameters, such as time constants (or 'residence times', when they relate to mixing processes, as in the present context) and gains which, in turn, determine a parameter known in climate science as the 'equilibrium climate sensitivity' (referred to simply as climate sensitivity and denoted by *CS* from hereon). The widely accepted definition of *CS* is the equilibrium change in global mean surface air temperature that would result from a sustained doubling of the atmospheric CO_2 concentration, where the radiative forcing required for this is likely to be about $5.35\ log_e(2) = 3.7\ W\ m^{-2}$ (Myhre, Highwood, Shine, & Stordal, 1998). Conveniently, the statistical estimates of the continuous-time model parameters do not depend on the sampling interval of the time series data and, of course, have the same physical connotations. As a result, it is normally possible to immediately interpret these differential equation models in relation to the physical nature of the system under investigation, as required by the DBM modelling philosophy (see chapter 12 in Young, 2011) and so, hopefully, add to their credibility in scientific terms.

The DBM model is not entirely formulated in continuous-time terms. Rather, it is a dynamic relationship that includes discrete-time models of the added stochastic and noise processes, so avoiding the problems associated with the estimation of purely stochastic continuous-time models. More specifically, it is a 'hybrid' version of the well-known, discrete-time Box-Jenkins model (Box & Jenkins, 1970) that is composed of a continuous-time transfer function relating the TRF to the GTA, and additive discrete-time noise represented by a standard ARMA process. This *Hybrid Box-Jenkins* (HBJ) model, as well as its estimation using a maximum likelihood approach, has been discussed in considerable detail in Young (2015) and is outlined later in Section 4.2. For the present purposes of forecasting the GTA, the HBJ model is contained within an over-arching *Unobserved Component* (UC) structure that contains another, time variable parameter, *Dynamic Harmonic Regression* (DHR) element (see later, Section 4) introduced to explain the presence of a pronounced quasi-cycle in the data that is not explained by the TRF input. By 'quasi-cyclic' I mean here that it is not a regular sinusoidal oscillation of constant frequency, phase

[1] This report can be downloaded from http://captaintoolbox.co.uk/Captain_Toolbox.html/Publication_Downloads.html as `Climate_DBM_Report.pdf`.

and amplitude but a non-stationary cyclic phenomenon in which all of these characteristics may change to some extent as time progresses. The extent of this variation is part of the DHR model identification and estimation procedure.

The main limitation of the DBM model and the associated forecasting procedure, as developed later in Sections 4 to 6 of the paper, is their reliance on this quasi-cyclic component which is more difficult to interpret in mechanistic terms. Consequently, Section 7 considers briefly how this initial DBM model might be developed further into a hypothetico-inductive DBM model (Young, 2013) form, where the non-stationary quasi-cyclic component is replaced by the introduction of the *Atlantic Multidecadal Oscillation* (AMO) series (Schlesinger, 1994) as a second explanatory input entering through a second continuous-time transfer function.

Before this, however, the next Section 3 considers the nature of more traditional, high order climate models and their emulation by a much lower order dynamic system. The emulation method used here is a special form of model reduction where the reduced order models capture the dominant modal behaviour of the large, higher order system and so are able to reproduce its dynamic behaviour almost completely (Young, 1999; Young & Ratto, 2009; Young et al., 1996). Note that more comprehensive details of this emulation analysis, as well as further details of the GTA modelling and forecasting analysis, are available in Young (2014) [2].

3. DBM emulation of large climate models

In order to justify the use of DBM model analysis and make it more widely acceptable, it seems advisable first to compare and contrast the resulting models with more conventional, climate simulation models. Such a comparison can help to explain better the nature of the DBM model, as it relates to the existing climate models, and allow for the evaluation of parameter values that have a prescribed physical meaning and a range of climatically acceptable values.

Probably the best known climate models are the large *Atmosphere-Ocean General Circulation Models* (AOGCMs), whose dynamic order is very high indeed, with internal mechanisms that are both complex and difficult to analyze in simple terms. The global average temperature response of a typical AOGCM model is shown as the grey dotted line in the two panels of Fig. 1 (see Stouffer and Manabe, 1994 for details). This is the response to a step-like TRF input (zero for 500 years, followed by a short ramp over 70 years to 3.7 W m^{-2} and then maintained at this level for 3880 years) with the average final level of the response reaching around 4.3 °C, and so revealing an equilibrium climate sensitivity of a similar value (see the definition of this parameter in the previous section). This model, designated GFDLR15a, was developed by the US National Oceanic and Atmospheric Administration, at the *Geophysical Fluid Dynamics Laboratory* (GFDL) and the response in both panels is compared with the response of two lower order emulation models, shown by the red lines.

The first emulation model response, shown in the left hand panel of Fig. 1, is generated by the *Model for the Assessment of Greenhouse Gas Induced Climate Change* (MAGICC) (e.g. Meinshausen, Raper, & Wigley, 2011) using a Matlab™ version of this model developed by Dr. David Leedal (*pers. comm.*). MAGICC has been considered successful in closely emulating AOGCM averaged outputs but, while it is small by the standards of the AOGCMs, it is still a rather large model composed of an interconnected set of 80 deterministic differential equations. For the present illustrative emulation purposes, no attempt has been made to optimize the parameters of this 80th order simulation model except that, in order to improve its comparison with the GFDL model response, the model response is multiplied by a small scale factor of 1.04, so effectively increasing its climate sensitivity of 4.15 °C (see below) to match reasonably that of the GFDL model: i.e. $CS = 1.04 * 4.15 = 4.32$ °C. All the other parameters are maintained at their nominal values, as provided by Dr. Leedal and listed in Young (2014).

For comparison, the right hand panel shows the response of the 1st order, 'nominal' DBM emulation model. This is a model that reproduces the behaviour of the large model for the specified set of large model parameters; whereas a 'full' emulation model is able to do the same but for a whole range of the large model parameter values (Young & Ratto, 2009, 2011). This first order model is estimated as follows:

$$\frac{dx(t)}{dt} = -0.00116x(t) + 0.643\frac{du(t)}{dt} + 0.00138u(t) + \eta(t) \quad (1)$$

where $x(t)$ is the global averaged temperature response, $u(t)$ is the TRF input and $\eta(t)$ is a noise variable. The annually sampled additive noise component $\eta(k)$ is identified as a discrete-time 6th order *Auto-Regressive* (AR) model. Such a stochastic model is required in this case because the simulated output of the AOGCM appears to have additive, coloured noise that cannot be accounted for by the effect of the deterministic input. Despite its low order, the *deterministic simulated* output of this model (i.e. taking no account of the AR(6) noise model) explains 99.6% of the GFDL model output variance and, not surprisingly, its associated climate sensitivity of $CS = 4.4$ °C is reasonably consistent with that of the GFDL and modified MAGICC models. Interestingly, a third order model identifies an additional damped oscillatory mode with a period of 90 years that helps to explain the small overshoot in the response that occurs in the first 100 years after the application of the step input, but this improvement is not sufficient to justify the additional four parameters.

This same kind of DBM emulation modelling analysis can also be applied to the simulated step response of the MAGICC model, although here both the simulated data and the emulation are totally deterministic. The analysis identifies an 8th order differential equation model that has time constants ranging from 0.275 to 650 years. This is

[2] This report can be downloaded from http://captaintoolbox.co.uk/Captain_Toolbox.html/Publication_Downloads.html as `HIDBM_Climate1.pdf`, but note that some of the analysis therein has been superseded by that presented here.

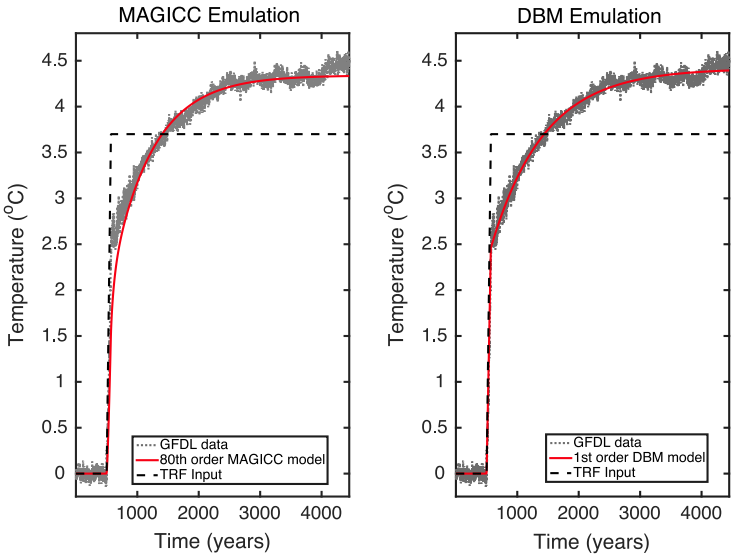

Fig. 1. GFDL model emulation by the MAGICC and 'nominal' DBM emulation models.

consistent with the range of time constants of the MAGICC model and it mimics the simulated response almost perfectly for any chosen input, such as the step inputs in Fig. 1 or the measured TRF input considered later in Section 5.

Moreover, and more importantly in the present context, even a 2nd order model is able to explain the MAGICC response well, with a coefficient of determination based on the simulated model output of $R_T^2 = 0.9999$; i.e. the simulated, deterministic output $x(t)$ of the model, which takes the following form,

$$\frac{d^2x(t)}{dt^2} + 0.02718\,\frac{dx(t)}{dt} + 3.884 \times 10^{-5}\,x(t) = 0.1753\,\frac{d^2u(t)}{dt^2} + 0.01432\,\frac{du(t)}{dt} + 4.384 \times 10^{-5}\,u(t), \tag{2}$$

explains 99.99% of the MAGICC model output variance. As explained later in Section 4.1, this model has two real eigenvalues that define the dominant modes of the model and their associated time constants (residence times in the present context) of 39 and 661 years. These, together with the steady state gain $G = 4.384/3.884 = 1.129\,^{\circ}\mathrm{C}/(\mathrm{W/m^2})$ and the associated climate sensitivity of $CS = G \times 3.7 = 4.15\,^{\circ}\mathrm{C}$ which, it will be noted, have physically meaningful units, clearly characterize the major aspects of the MAGICC model's dynamic behaviour and almost completely explain its response to the input TRF. In fact, the steady state gain G could be considered as a more obvious measure of climate sensitivity than CS.

While the above DBM emulation modelling results are interesting in their own right, their consideration in the present paper is primarily because they show how the dynamic response of high order climate models and systems can be reproduced almost exactly by low order DBM emulation models. Indeed, this is the main reason why any attempt at directly estimating the parameters of the high order system encounters serious identification problems and requires some form of constrained optimization: there is just not enough information in the observed data to identify anything more than that associated with the dominant dynamic modes, as revealed by the reduced order model.

Dominant modal behaviour, such as that we see in the above climate simulation examples, is obviously the reason also why Hasselmann, Hasselmann, Giering, Ocana, and Storch (1997) and Hasselmann, Sausen, Maier-Reimer, and Voss (1993) found that the simulated response to radiative forcing of the ECHAM3 climate model was captured by the sum of just three first order exponential terms; whilst Hooss, Voss, Hasselman, and Maier-Reimer (2001) and Lowe (2003) found that, in the case of both the ECHAM3 and HadCM3 models, the response was captured by the sum of two first order exponential terms. In other words, the dominant modal behaviour is the main influence on the observed globally averaged response of the high order climate models and it is clear, therefore, that any study seeking to identify a stochastic model of the actual globally averaged temperature variations for the purposes of short to medium term forecasting or emissions management should acknowledge this. More specifically, it should seek an identifiable, low order DBM model that captures the dominant modal behaviour *in the observed data*, for this is the primary objective of the forecasting, and is also optimal in statistical terms.

4. DBM model identification and estimation

In the present climate forecasting context, the generic DBM model takes the following *Unobserved Component* (UC) form (see e.g. Pedregal and Young, 2002):

$$y(k) = T(k) + C(k) + f\{\mathbf{u}(k)\} + e(k). \tag{3}$$

Here the argument k denotes that the associated variable is sampled at the kth sampling instant; $y(k)$ is the output variable to be forecast, in the present context the GTA; $T(k)$

is a 'trend' component, reflecting any longer term, non-stationary movements in $y(k)$ *that are not accounted for by such behaviour in the inputs* $\mathbf{u}(k)$; $C(k)$ is a cyclical or quasi-cyclical component representing any such effects present in $y(k)$; $f\{\mathbf{u}(k)\}$ models the effect on $y(k)$ of any inputs or exogenous variables, represented by the vector $\mathbf{u}(k)$; and $e(k)$ is an 'irregular' component that allows for stochastic effects that are not modelled by the other components and, in the best of circumstances, will be a zero mean, serially uncorrelated sequence of random variables ('white noise'). It is important to note that, in the climate example considered in Section 5, the trend component $T(k)$ is not required because the trend-like behaviour in $y(k)$ is, indeed, present in the behaviour in the TRF input $u(k)$.

In general, the effect of inputs $\mathbf{u}(k)$ could be quite simple, for instance via a static regression relationship in several variables; or it could be a dynamic effect, with each input entering via a linear or state-dependent parameter (Young, 2000), nonlinear *Transfer Function* (TF), representing discrete or continuous-time dynamic relationships and depending on the nature of the system. If a continuous-time transfer function is used, then $f\{\mathbf{u}(k)\}$ is the deterministic output of this model sampled at the kth sampling instant. In forecasting terms, such inputs should be available as 'leading indicators' over the forecasting interval, or they will have themselves to be forecast over this interval. In the latter case, each input $u_i(k)$ would need to be modelled and forecast; in which case the same kind of UC type model (3) can be used, this time omitting the $f\{\mathbf{u}(k)\}$ component, i.e.,

$$u_i(k) = T_i(k) + C_i(k) + e_i(k) \tag{4}$$

for each input $u_i,\ i = 1, 2, \ \ldots, p$. In the present paper, we are concerned mainly with a single input, the radiative forcing TRF, measured in W/m^2, that does not include any cyclical or quasi-cyclical components. Of course, the same basic approach can be used if the TRF is decomposed into some, or all, of its constituent components and these are considered as separate inputs entering through transfer functions (see section 6 of Young & Jarvis, 2002 where this approach is used to allow for the study of emissions control and management).

When it is required, as it is in the case of the TRF input $u(k)$, the trend component $T(k)$ is assumed to be a non-stationary process that characterizes the long-term changes in the level of the series by a random walk model from the *Generalized Random Walk* (GRW) family (see chapter 4 in Young, 2011) that includes the *Random Walk* (RW), *Integrated Random Walk* (IRW) and *Smoothed Random Walk* (SRW) as special cases. The cyclical term $C(k)$ is modelled as the following a *Dynamic Harmonic Regression* (DHR):

$$\text{Cyclical}: \quad C(k) = \sum_{i=1}^{R_s} \{\alpha(i,k)\cos(\omega_i k) + \beta(i,k)\sin(\omega_i k)\} \tag{5}$$

where each $\alpha(i,k)$ and $\beta(i,k)$ is a stochastic *Time Variable Parameter* (TVP), again modelled by one of the GRW family; and $\omega_i,\ i = 1, 2, \ldots, R_s$, are the fundamental and harmonic frequencies associated with the identified periodicity in the series (see the full description in Young, Pedregal, & Tych, 1999). These frequency values are chosen by reference to the spectral properties of the time series, as revealed by its AR spectrum (Priestley, 1981) identified using the *Akaike Information Criterion* (AIC) (Akaike, 1974). The time variability of the $\alpha(i,k)$ and $\beta(i,k)$ parameters in (5) is determined by two 'hyper-parameters' that are associated with each of the model parameters in the GRW model. These are the *Noise Variance Ratio* (NVR) and the 'damping' (alpha) values that control the rate of change of the level and slope of the TVP. The DHR analysis uses the recursive *Kalman filter* (KF) and *Fixed Interval Smoothing* (FIS) algorithms to estimate the unobserved components, with the associated hyper-parameters optimized in order to minimize the least squares error between the pseudo-spectrum of the DHR model and the empirical AR spectrum of the $y(k)$ series.

Modelling in these general UC terms is possible using the combination of two routines available in the CAPTAIN Toolbox [3] for Matlab™: the DHR algorithm, provided by the dhr routine; and the *Refined Instrumental Variable* (RIV) group of routines provided, in the present context, by the rivcbjid and rivcbj routines for the identification and estimation of continuous-time transfer function models.[4] These relate directly to differential equation relationships, as considered in the next two Sections 4.1 and 4.2.

Finally, it is worth noting that, although the DHR model in Eq. (5) is specified in discrete-time at the same sampling interval as the measured data, it can be considered as a continuous-time representation of these data because of the sine and cosine terms which are continuous-time objects. In fact, the output of the DHR model could be sampled at a faster of slower rate than the sampling interval of the measured data, if required, although this option is not currently available in the CAPTAIN dhr routine.

4.1. Differential equation models

A typical, continuous-time DBM model is normally presented in a useful continuous-time transfer function form but, to start with, it will be considered also in the equivalent differential equation form that may be more familiar to a wider audience. In the case where a single output variable $x(t)$ is related to nu input variables $u_i(t),\ i = 1, 2, \ \ldots, nu$, the simplest model takes the following general form:

$$\frac{d^n x(t)}{dt^n} + a_1 \frac{d^{n-1}x(t)}{dt^{n-1}} + \cdots + a_n x(t) = \sum_{i=1}^{nu} b_{i0} \frac{d^{m_i} u_i(t-\tau_i)}{dt^{m_i}} + \cdots + b_{im_i} u_i(t-\tau_i) \tag{6}$$

where $\tau_i,\ i = 1, 2, \ \ldots, nu$ are pure time delays to allow for any such delays in the system dynamics; while $a_j,\ j = 1, 2, \ \ldots, n$ and $b_{ij},\ i = 1, 2, \ \ldots, nu;\ j = 0, 2, \ \ldots, m_i$ are normally constant parameters. A model such as this can

[3] The CAPTAIN Toolbox is freely available via the website http://captaintoolbox.co.uk/Captain_Toolbox.html/Captain_Toolbox.html.

[4] Equivalent rivbjid and rivbj routines are available if discrete-time models are preferred.

be transformed straightforwardly into an equivalent state-space form. More importantly in the present context, it can also be written as a TF model in the equivalent 'common denominator' operator form Young (2011):

$$x(t) = \sum_{i=1}^{nu} \frac{b_{i0}s^{m_i} + b_{i1}s^{m_i-1} + \cdots + b_{im_i}}{s^n + a_1 s^{n-1} + \cdots + a_n} u_i(t-\tau_i) = \sum_{i=1}^{nu} \frac{B_i(s)}{A(s)} u_i(t-\tau_i) \quad (7)$$

where s^r is the derivative operator, i.e. $s^r = d^r/dt^r$, while $\{B_i(s);\ A(s)\}$, $i = 1, 2, \ldots, nu$, are the appropriately defined polynomials in this operator. The model can be extended easily to additive TFs with different denominators, i.e. where $A(s)$ in (7) is replaced by $A_i(s)$. And a multi-output system can be defined as an amalgamation of single output models such as this.

Eq. (2) is a simple example of (7) with $nu = 1$, $n = 2$, $m = 3$ and $\tau = 0$. Its TF equivalent is

$$x(t) = \frac{0.01753s^2 + 0.01432s + 4.384 \times 10^{-5}}{s^2 + 0.02718s + 3.884 \times 10^{-5}} u(t) = F(s)u(t) \quad (8)$$

where the denominator $s^2 + 0.02718s + 3.884 \times 10^{-5}$ of the transfer function $F(s)$ can be factored into two terms defined by its real roots, so that

$$F(s) = \frac{0.01753s^2 + 0.01432s + 4.384 \times 10^{-5}}{(s + 0.0257)(s + 0.00151)}. \quad (9)$$

Then, using partial fraction expansion (Young, 2011), the transfer function $F(s)$ can be decomposed to the form:

$$F(s) = \frac{0.00862}{s + 0.0257} + \frac{0.000935}{s + 0.00151} + 0.175 = \frac{0.336}{1 + 39.0s} + \frac{0.618}{1 + 661s} + 0.175 = \frac{G_1}{1 + T_1 s} + \frac{G_2}{1 + T_2 s} + G_I. \quad (10)$$

This means that the model has a 'parallel-pathway' decomposition in which the total output response is the sum of the outputs from the two first order transfer functions and the instantaneous mode G_I (i.e. the immediate response $G_I u(t)$ at the output, following a change in the input variable $u(t)$).

It is easy to calculate the physically meaningful characteristics of the model from these TF equations:

1. The steady state gains G_1, G_2 and G_I determine the steady state level of the response to a unit step input. Consequently, they are obtained when there is no further change in the response to this input, i.e. when $s = d/dt$ is set to zero in the TF: for instance, the overall steady state gain from (8) is $G = 4.384 \times 10^{-5}/3.884 \times 10^{-5} = 1.129\ ^\circ\text{C}/(\text{W/m}^2)$ so that, in this case, the nominal $2 \times CO_2$ climate sensitivity for this model is $CS = 3.7G = 4.15\ ^\circ\text{C}$.
2. From (10), the instantaneous effect of the radiative forcing is $G_I = 0.175\ ^\circ\text{C}$; while the two modes have steady state gains of $G_1 = 0.336\ ^\circ\text{C}/(\text{W/m}^2)$ and $G_2 = 0.618\ ^\circ\text{C}/(\text{W/m}^2)$, respectively (note that $G = G_I + G_1 + G_2$), with associated time constants of $T_1 = 39$ and $T_2 = 661$ years, respectively. This means that the radiative forcing input has three effects on the temperature, as determined by the 'partition percentage' PP_i in each case: the instantaneous effect, with $PP_I = 100 \times G_I/G = 15.5\%$; the 'quick' effect $PP_q = 100 \times G_1/G = 29.8\%$; and the very long term 'slow' effect $PP_s = 100 \times G_2/G = 54.7\%$:

4.2. The hybrid Box-Jenkins model

The specific TF model used for the DBM modelling is the following *Hybrid Box-Jenkins* (HBJ) model, which follows from the original, fully discrete-time model introduced by Box and Jenkins (1970). It is simply a stochastic version of the TF model (7) with different denominators and an additional, coloured noise component modelled as the well known discrete-time ARMA process (see Young, 2011; Young, 2015 for a full description of the HBJ model and its optimal estimation). This model can be written informally in the following decomposed hybrid form:

$$\begin{aligned} \text{Deterministic Model}: \quad & x(t) = \sum_{i=1}^{nu} \frac{B_i(s)}{A_i(s)} u_i(t-\tau_i) \\ \text{Noise Model}: \quad & \xi(k) = \frac{D(z^{-1})}{C(z^{-1})} e(k); \quad e(k) = \mathcal{N}(0, \sigma^2) \\ \text{Observation Equation}: \quad & y(k) = x(k) + \xi(k) \end{aligned} \quad (11)$$

where $x(k)$ is the sampled value of $x(t)$ at the kth sampling instant and $e(k)$ is a zero mean white noise input, while $C(z^{-1})$ and $D(z^{-1})$ are the following polynomials:

$$\begin{aligned} C(z^{-1}) &= 1 + c_1 z^{-1} + c_2 z^{-2} + \ \ldots\ + c_p z^{-p} \\ D(z^{-1}) &= 1 + d_1 z^{-1} + d_2 z^{-2} + \ \ldots\ + d_q z^{-q}. \end{aligned} \quad (12)$$

Here z^{-r} is the backward shift operator, i.e. $z^{-r}\xi(k) = \xi(k-r)$. This nomenclature is used here because it appears in the cited references on DBM modelling, where it arises from the relationship between the backward shift and discrete-time z operator theory. In time-series analysis, however, Box and Jenkins use of B (which would conflict with the use here of B in the transfer function model); while in econometrics L (for 'Lag') is favoured; and, finally, in control systems identification, z^{-r} is often replaced by q^{-r}. The full model structure is defined by [n im_i ($i = 1, 2, \ldots, nu$) τ_i ($i = 1, 2, \ldots nu$) p q] and identification of the model structure parameters that define this vector, as well as the estimation of the polynomial parameters (a_i, $i = 1, 2, \ldots, n$, $b_{i,j}$, $i = 0, 1, \ldots, m_i$; $j = 1, 2, \ldots, nu$, c_i, $i = 1, 2, \ldots, p$, d_i, $i = 1, 2, \ldots, q$ and σ^2) that characterize the associated model, is solved using an iterative 'pseudo-linear regression' approach to maximum likelihood optimization (Young, 2015) that is coded in the rivcbjid and rivcbj routines of the CAPTAIN Toolbox.

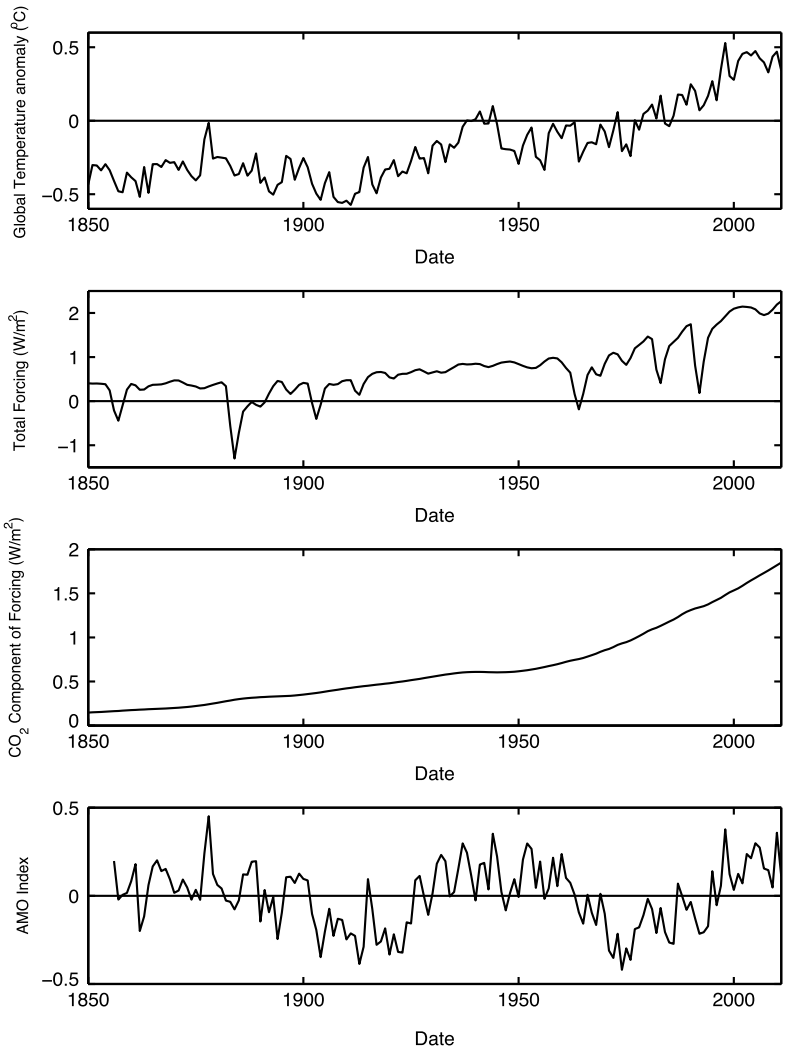

Fig. 2. Globally averaged climate data. Top panel: *Global Temperature Anomaly* (GTA), from the Carbon Dioxide Information Analysis Center (CDIAC) in 2009. Second and third panels: *Total Radiative Forcing* (RTF) signal and the CO_2 component of this total signal, from the Potsdam Institute for Climate Impact Research website. Lower panel: AMO series, downloaded from the Physical Sciences Division, Earth System Research Laboratory of NOAA.

5. DBM modelling and forecasting global average temperature

In this example, the main objective is the DBM modelling and short term forecasting of the *Global Temperature Anomaly* (GTA). The annual anomalies here are the difference between the current globally averaged surface temperature and the average of this temperature recorded from 1951 to 1980, thus showing whether the temperature is warmer or cooler than this reference period. In this regard, previous research and development studies on forecasting applications have shown that the UC models such as (3) and (4) yield good forecasting performance when used within a suitable forecasting engine, such as a modified Kalman Filter (see e.g. Young, 2010 and the prior references therein, where such models are used in flow forecasting), or its equivalent transfer function form, as used in the present paper.

5.1. DBM modelling

The DBM modelling and forecasting studies outlined in this and subsequent Sections 6 and 7 are based on the statistical analysis of the annual, globally averaged climate data plotted in Fig. 2 from 1850 up to the start of the new Millenium in 2001, thus allowing for short-term forecasting over the next ten years to the end of the full data set in 2011,[5] as well as with some recently acquired GTA measurements from 2012 to 2015 (see later). These

[5] Data download sites: http://cdiac.ornl.gov/trends/temp/jonescru/jones.html; http://www.pik-potsdam.de/~mmalte/rcps/; http://www.cgd.ucar.edu/cas/catalog/climind/AMO.html. Note: The data from these sites were accessed in 2009, when the present study was initiated, and they can change, so the GTA, RTF and AMO data sets used in the present paper can be downloaded as Climate Data.zip from http://captaintoolbox.co.uk/Captain_Toolbox.html/Publication_Downloads.html.

short-term forecasts are also extended to 50 years for illustrative purposes.

The first step in the DBM approach is always the definition of the modelling objectives. In the present case these are to obtain a well-identified model that makes sense in climatic terms, adequately explains the estimation data set and provides good short-term forecasts up to at least 10 years ahead. The model identification and estimation analysis considered first is based on the 152 annual samples of the measured RTF and GTA data from 1850 to 2001 and it does not involve any forecasting. The first step is the definition of the model and the statistical identification of its dynamic order. Based on physical considerations and supported by the causality analysis of Stern and Kaufmann (2014), it makes sense to consider the dynamic relationship between the forcing input TRF, denoted by $u(t)$, and the GTA output, denoted by $x(t)$. Using the HBJ model form in (11), the order identification procedure applied to the yearly sampled data $\{y(k), u(k)\}$, $k = 1, 2, \ldots, 152$, is fairly standard: a range of possible model orders are investigated and evaluated in relation to well known model order identification criteria such as the AIC and the *Bayesian Identification Criterion* (BIC) (see e.g. Section 5.4.5 of Priestley, 1981) using, in this example, the CAPTAIN routine rivcbjid which incorporates such criteria. This quite clearly identifies two possible first order [1 2 2 0 0 1 0] models of the HBJ type, i.e.

$$y(k) = \frac{b_{11}s + b_{12}}{s + a_1}u(k) + \frac{b_{21}s + b_{22}}{s + a_2}u_{IC}(k) + \frac{1}{1 + c_1 z^{-1}}e(k), \tag{13}$$

one with $a_1 \neq a_2$ and the other with common denominators and $a_1 = a_2$. This equation is written here informally as a single 'snapshot' equation in hybrid operator form, with the argument k now indicating the sampled value of the variables associated with the underlying continuous-time model. The second input $u_{IC}(k) = 1.0\,\forall\, k$ is introduced simply to handle any significant initial conditions. This is based on Laplace transform theory [6] and its inclusion is important in data such as these where the initial condition effect is considerable and estimation without allowing for it in this manner yields poor results. The alternatives are to remove the initial condition effects by either differencing or detrending the data. Differencing does not work in this case because it has the undesirable side effect of amplifying the high level of noise in the data and totally obscuring the input–output relationship. Detrending depends on the subjective judgement required to select the detrending method (linear, quadratic, stochastic?) and, in any case, incorporating the estimation of initial conditions is easy and appears to work better.

Of the two model structures identified, the common denominator model is estimated by rivcbj; while the other with different denominators is estimated using the alternative CAPTAIN routine rivcdd, both using the sampled data $\{y(k), u(k)\}$, $k = 1, 2, \ldots, 152$. The two models are reasonably similar in stochastic terms, with serially uncorrelated residuals $e(k)$ that do, however, have some undesirable correlation with the input variable $u(k)$. As might be expected, the one with different denominators explains the GTA data a little better: it has a coefficient of determination based on the error $\hat{\xi}(k) = y(k) - \hat{x}(k)$, where $\hat{x}(k)$ is *the sampled, deterministic output of the TF model*, of $R_T^2 = 0.80$, compared with $R_T^2 = 0.78$ for the TF with the same denominator. In both cases, however, the explanation is better than that provided by the MAGICC and emulation models discussed in Section 3 where, when the unit step forcing there is replaced by the actual forcing $u(k)$ here, the $R_T^2 = 0.75$.

The main problem with these initial transfer function models is the rather high variance of the noise $\xi(k)$, which also appears visually to have some long-term fluctuations. Although the AIC identifies the AR(1) noise model, there is a notable dip in the criterion at AR(29), suggesting some increase in the information at this high order. The associated AR(29) spectrum is characterized by $R_s = 13$ peaks, with two large, low frequency peaks at periods of 46.9 and 19.3 years/cycle. In addition to this, there is a large peak at 3.6 years/cycle and lesser peaks with periodicities of 9.2, 6.1, 4.9, 4.2, 3.2, 2.8, 2.6, 2.3, 2.1 and 2 years/cycle, respectively. The DHR model based on this AR(29) spectrum, as estimated using the CAPTAIN dhropt and dhr routines, explains $\xi(k)$ well, with a coefficient of determination, this time based on the final stochastic residuals, of $R^2 = 0.90$

When combined, the 46.9 year and 19.3 year cycles estimated by the DHR model can be considered to form a long period 'quasi-cycle'. This term is used because the estimated time variable parameters in the DHR model mean that the cycles do not have constant amplitudes, periods and phase characteristics. Rather the estimated cyclicity exhibits changes in these characteristics around the 'average' estimated period in a manner defined by the optimized hyper-parameters of the DHR model (see the discussion on DHR estimation in Young and Pedregal, 1999). In forecasting terms, therefore, we should expect the quasi-cycle, as estimated and forecast by the DHR model, to change with the sample size. At any sample k, however, it will be projected forward as a constant parameter DHR model with the frequency, sine and cosine parameter values, $\omega_i k$, $\alpha(i, k)$ and $\beta(i, k)$, $i = 1, 2, \ldots, 13$ set to those estimated at sample k.

The initial identification and estimation results obtained above suggest a full UC model, incorporating the quasi-cyclic component $C(k)$, of the form:

$$\begin{aligned} \text{TF Model}: \; & x(t) = \frac{b_{11}s + b_{12}}{s + a_1}u(t) + \frac{b_{21}s + b_{22}}{s + a_2}u_{IC}(t) \\ \text{Cyclical}: \; & C(k) = \sum_{i=1}^{13} \{\alpha(i, k)\cos(\omega_i k) + \beta(i, k)\sin(\omega_i k)\} \\ \text{Noise}: \; & \xi(k) = e(k); \quad e(k) = \mathcal{N}(0, \sigma^2) \\ \text{Output}: \; & y(k) = x(k) + C(k) + e(k). \end{aligned} \tag{14}$$

The complete optimization of the above UC model requires concurrent estimation of the periodic and transfer function components, again from the same sampled

[6] See http://captaintoolbox.co.uk/Captain_Toolbox.html/Technical_Matters/Entries/2012/10/18_Estimating_Initial_Conditions.html and Young (2014).

Table 1
Optimized hyper-parameters for DHR model of the quasi-cyclic component $C(k)$.

Period (yrs)	48.0	19.3	9.2	6.1	4.9	4.2	3.6
NVR	0.041	0.023	0.027	0.005	0.044	0	0.005
alpha	0.976	0.962	0.952	0.969	0.923	0.022	0.995

Table 2
Table 1 continued.

Period (yrs)	3.2	2.8	2.6	2.3	2.1	2.0
NVR	0.0004	0.0014	0.0013	0	0.0003	0.0017
alpha	0.982	0.981	0.982	0	0.981	0.985

data $\{y(k), u(k)\}$, $k = 1, 2, \ldots, 152$ used in the initial model identification. This is achieved by an iterative procedure known as 'backfitting' (Pedregal & Young, 2002), in which the time domain optimization of the RIV algorithm is combined with frequency domain optimization of the DHR algorithm. In particular, at each iteration the periodic components are estimated by the dhr routine based on the noise series $\hat{\xi}(k) = y(k) - \hat{x}(k)$ from the previously estimated transfer function model, so that the DHR estimates are conditional on its estimated parameters. In this example, convergence appears to be complete after two iterations. The resulting estimates of the main TF model parameters are as follows:

$$\begin{aligned} &\hat{a}_1 = 0.0518(0.004);\ \hat{a}_2 = 0.0193(0.008);\\ &\quad \hat{b}_{11} = 0.0626(0.002)\\ &\hat{b}_{12} = 0.0363(0.003);\ \hat{b}_{21} = -0.369(0.010);\\ &\quad \hat{b}_{22} = -0.012(0.001);\\ &\hat{\sigma}^2 = 0.001; \end{aligned} \tag{15}$$

where the figures in parentheses are the estimated standard errors. The time variable parameters of the $C(k)$ model are defined by their estimated values at sample $k = 1, 2, \ldots, 152$. The only change in the AR(29) spectrum associated with the finally estimated quasi-cycle, in comparison with the initial estimation, is in the lowest frequency peak, whose period increases a little from 46.9 to 48.0 years/cycle. The optimized NVR and alpha hyper-parameters of the DHR model (see Section 4) are given in Tables 1 and 2. The model is evaluated statistically in the normal manner, with checks on the correlation properties of the residual error; and it is validated, in the present context, by forecasting exercises, as discussed in the next Section 6.

Not surprisingly, the addition of the quasi-cycle to the model makes a considerable difference. The lower panel of Fig. 3 compares the model output with the measured GTA data over the period from 1850 to 2001 and we see that it has captured the major movements in temperature over these 152 years, with a coefficient of determination based on the final model residuals $e(k)$ of $R^2 = 0.976$. These residuals are plotted in the upper panel: they have zero mean value with $\sigma^2 = 0.001$; and they are both serially uncorrelated and uncorrelated with the input $u(k)$, as required. The upper panel of Fig. 4 is similar to the main panel of Fig. 3 but the lower panels reveal the hidden 'unobserved components' of the model response by decomposing it into the response of the main TF component, the initial condition response and the quasi-cycle. The full estimated quasi-cycle is shown as the black line, while the dash-dot line is the sum of its two long period components.

The model evaluation is not complete, however, because the DBM modelling procedure also requires the physical characteristics of the model to make reasonable sense and to be credible in climatic terms. The most important part of the model in this regard is the TF $F_1(s)$ between the TRF $u(t)$ and the temperature $x(t)$, i.e.,

$$\begin{aligned} F_1(s) &= \frac{b_{11}s + b_{12}}{s + a_1} = b_{11} + \frac{b_{12} - (b_{11}a_1)}{s + a_1}\\ &= K_1 + \frac{G_1}{1 + T_1 s} \end{aligned} \tag{16}$$

where the estimated physical parameters are the instantaneous gain, $K_1 = b_{11} = 0.0626\ ^\circ\text{C}/(\text{W/m}^2)$; the gain of the TF, $G_1 = (b_{12}/a_1) - b_{11} = 0.6376\ ^\circ\text{C}/(\text{W/m}^2)$; and the residence time $T_1 = 1/a_1 = 19.31$ years. The associated climate sensitivity is computed from the total gain $G = b_{12}/a_1 = 0.7\ ^\circ\text{C}/(\text{W/m}^2)$ (note that $G = K_1 + G_1$), so that $CS = 3.7G = 2.59\ ^\circ\text{C}$. However, because these are not estimated directly but derived from the estimated TF model parameters via nonlinear transformations, their uncertainty is obtained from probability distributions estimated using Monte Carlo analysis, based on 10,000 stochastic realizations, and the estimated error covariance matrix of the directly estimated parameters. The resulting 68.2 percentile ranges are as follows:

$$\begin{aligned} &\hat{T}_1 = 18.7 \rightarrow 19.9 \text{ years};\\ &\quad \hat{G} = 0.67 \rightarrow 0.73\ ^\circ\text{C}/(\text{W/m}^2);\\ &\quad\quad \hat{CS} = 2.47 \rightarrow 2.71\ ^\circ\text{C} \end{aligned} \tag{17}$$

and, for later reference, the 95 percentile range for $\hat{CS} = 2.21 \rightarrow 3.04$. Note that $\hat{CS}$ is within the usually accepted range of 1.5–4.5 (e.g. Cubasch, 2001); moreover, it agrees reasonably with the lower values obtained using econometric time series analysis (see e.g. Kaufmann et al., 2006a; Mills, 2009, where the former range from 1.7 to 3.5 and the latter gives an estimate of 2.16 ± 0.44). As a reviewer pointed out, uncertainty bounds such as these that are associated with imperfect fit to the data are often neglected by climate modellers in other efforts to derive climate sensitivity from the observational record (see e.g. Knutti & Hegerl, 2008).

The estimated residence time is significantly different from the 39 year time constant that dominates the

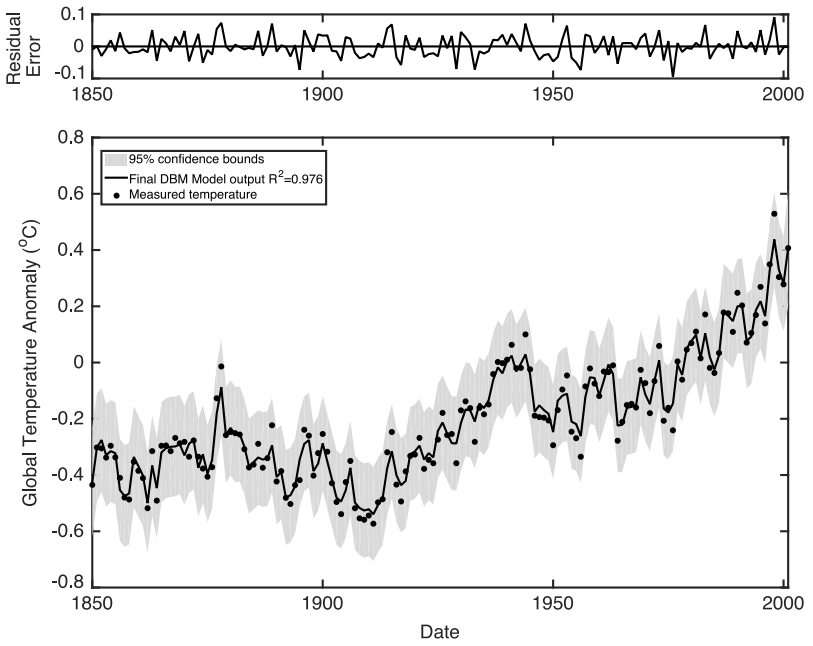

Fig. 3. Estimated deterministic output $\hat{y}(k) = \hat{x}(k) + \hat{C}(k)$ of the full DBM model (14) compared with the measured GTA $y(k)$, with the residual error $e(k)$ shown above.

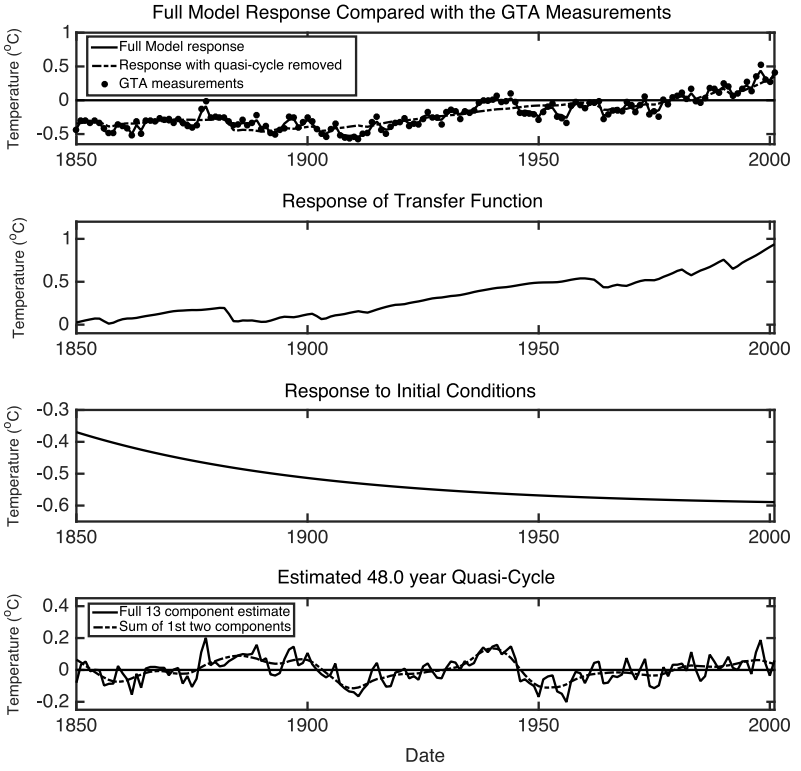

Fig. 4. Contributions to the DBM model response: complete response $\hat{y}(k)$, in the top panel, compared with the measured GTA $y(k)$ and the response with the quasi-cycle removed. The various estimated components of $\hat{y}(k)$ are plotted below this.

dynamic behaviour of the second order DBM emulation of the MAGICC model (Eq. (2)). However, it must be recalled that the MAGICC model used here is based on a nominal set of parameters and it does not explain the GTA as well as the TF part of the DBM model (i.e. the first-stage model that does not include the quasi-cycle component).

Table 3
Optimized hyper-parameters for DHR model for total radiative forcing $u(t)$.

Component	Long-term trend	9.2 years	4.9 years	3.1 years
NVR	0.26	0.77	0.12	7.7×10^{-6}
alpha	0.43	0.86	0.90	0

The inclusion of the quasi-cycle in the DBM model not only improves its ability to explain the GTA; as we shall see later in Section 7, it also has climatic credibility in the sense that it is of a similar period and nature to the quasi-cyclic behaviour of the AMO series shown in the lowest panel of Fig. 2. And while the estimated climate sensitivity of 2.59 °C is quite different to the 4.15 °C for the MAGICC emulation model, this is a notoriously uncertain measure and both values lie within the usually accepted range. Moreover, the difference in *CS* estimates probably accounts for the poorer performance of the MAGICC model and suggests that the DBM model value of 2.59 is a more reliable estimate. So we can conclude that the model (14) is acceptable from a DBM modelling standpoint.

Finally, it is interesting to compare the DBM modelling results with those of Mills (2010), who uses a 'structural model' approach to time-series modelling to consider the relationship between radiative forcing and the GTA. The structural model is a discrete-time model of the UC type but Mills does not include a transfer function component, nor does he note the presence of the quasi-cycle, which is absorbed in the trend component. Consequently, as he says in relation to his estimated model, "The trend component is generated as a random walk process with no drift, so that a pronounced warming trend cannot be forecast". By including the TF and quasi-cyclic models in the DBM model, however, it is now possible to consider forecasting the GTA, as discussed in the next section, and examine whether a warming trend is likely to continue, at least in the short to medium term.

6. Short and medium-term forecasting

The stochastic DBM model (14) provides an excellent basis for forecasting. This section discusses briefly the forecasting methodology and then shows how it is able to forecast the GTA very well over the 14 years from 2001 to 2014, with credible forecasts after this. It also shows how the model can be used successfully in 10-year-ahead 'rolling forecasts' of the data before 2001.

6.1. Forecasting the components of the DBM model

Since the model (14) is additive in form, the forecasting system is in three main parts: forecasting (i) the radiative forcing input $u(t)$; (ii) the output $\hat{x}(t)$ of the TF model using this input forecast; and (iii) the quasi-cycle $\hat{C}(k)$ based on the error between the $y(k)$ and $\hat{x}(k)$ up to the forecasting origin. The first and last tasks are achieved using DHR forecasting based on the standard discrete-time Kalman Filter Young et al. (1999), while task (ii) exploits a transfer function form of the Kalman Filter. The results of the forecasting analysis for the three components are presented and discussed in the next three sections. The forecast of the total GTA $\hat{y}(k+f|k)$, where f is the forecast interval, is then obtained as the sum of the $\hat{x}(k+f|k)$ and $\hat{C}(k+f|k)$ forecasts, as discussed in Section 6.1.4.

6.1.1. DHR forecasting the forcing input

In this case, the AIC applied to the radiative forcing signal $u(t)$ suggests an AR(7) model and the associated spectrum has a strong trend component, with very shallow peaks 9.2, 4.9 and 3.1 year periods, showing that the perturbations about the trend, due to phenomena such as volcanic eruptions, are too random in occurrence to exhibit any clear, forecastable patterns. The resulting DHR model is a SRW trend plus three quasi-cycles, with the hyper-parameters optimized using dhropt. This yields the optimal hyper-parameters in Table 3 and the forecasting results are shown in Fig. 5. Here, the DHR estimate is the deterministic output of the model (see figure caption) plotted up to 2001, with the 50 year ahead forecast plotted thereafter. The latter forecast is dominated by the SRW trend and this seems quite reasonable given the irregular nature the big dips in the historical series that are the results of major volcanic eruptions (Mt Agung, 1963; El Chichon, 1982; Mt Pinatubo, 1991; Mt Krakatoa, 1883). Also plotted in Fig. 5, for comparison, is the forecast produced using a more conventional *AutoRegressive Integrated Moving Average* (ARIMA) model: this is discussed further in Section 6.3.

6.1.2. DHR forecasting the quasi-cycle

Although based on a more complex model, the DHR forecast of the quasi-cycle uses exactly the same forecasting procedure as that used for the radiative forcing input. The DHR modelling and hyper-parameter optimization have been discussed in Section 5.1 and the forecasts based on this model are shown in Fig. 6. The red dash-dot line is the sum of the first two, longer-term components which explain quite a lot of the variation. The initial negative forecasts after 2001 are important, as discussed in Section 6.1.4.

6.1.3. Forecasting the Hybrid BJ model output

Extending the analysis of Young (1979), which considers the transfer function form of the Kalman Filter, a 'snapshot' of a single input HBJ model can be written in the following forecasting form, where $x(k+1)$ is the sampled output of the continuous-time TF model at the $(k+1)$th sampling instant:

$$y(k+1) = x(k+1) + \frac{D(z^{-1})}{C(z^{-1})}\{y(k+1) - \hat{y}(k+1|k)\} \quad (18)$$

while $\hat{y}(k+1|k)$ is the one step ahead forecast output. Solving for $\hat{y}(k+1|k)$, we obtain the one step ahead forecasting equation:

$$\hat{y}(k+1|k) = \hat{x}(k+1) + \frac{D(z^{-1}) - C(z^{-1})}{D(z^{-1})} \times \{y(k+1) - \hat{x}(k+1)\} \quad (19)$$

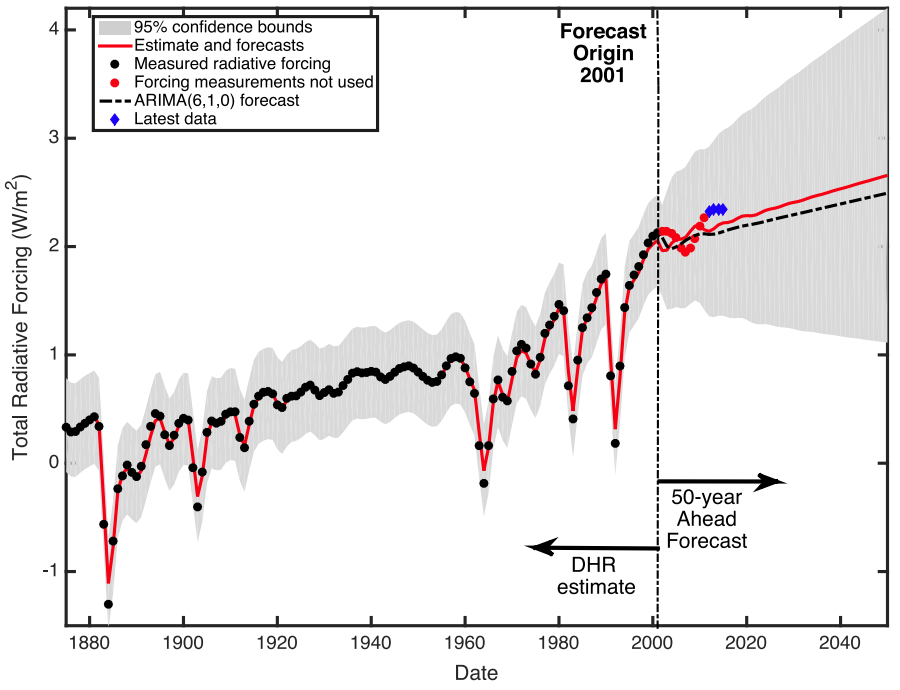

Fig. 5. DHR model estimation results and 50 year DHR and ARIMA model forecasts of the TRF input signal from 2001. (For interpretation of the references to colour in this figure legend, the reader is referred to the web version of this article.)

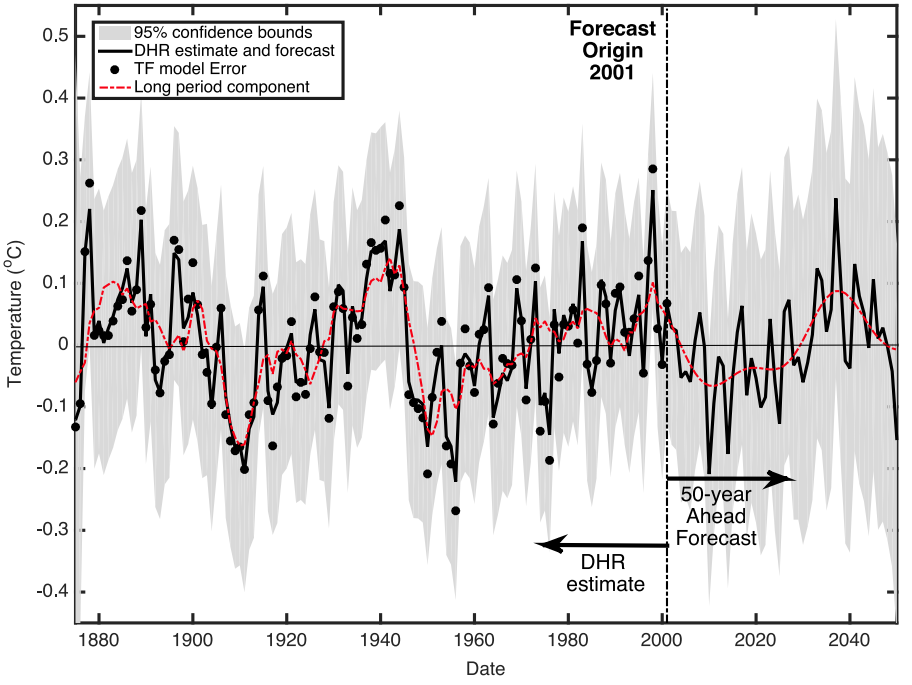

Fig. 6. DHR estimation and 50 year forecast of the quasi-cyclic component from 2001. (For interpretation of the references to colour in this figure legend, the reader is referred to the web version of this article.)

where $\hat{x}(k+1)$ is now the one step ahead forecast of the continuous-time TF component of the DBM model in Eq. (14). The multi-step ahead forecasts of $y(k+f|k)$ are generated in the usual manner. Note that the $D(z^{-1}) - C(z^{-1})$ term means that $y(k+1) - \hat{x}(k+1)$ is being operated upon by one or more backward shifts and no direct term, so it only refers to past errors of this kind and does not involve any future values of $y(k)$. Also, in the case of white noise, where $C(z^{-1}) = D(z^{-1}) = 1.0$, we see that the forecasting is particularly simple with $\hat{y}(k+f|k) = \hat{x}(k+f|k)$ so that,

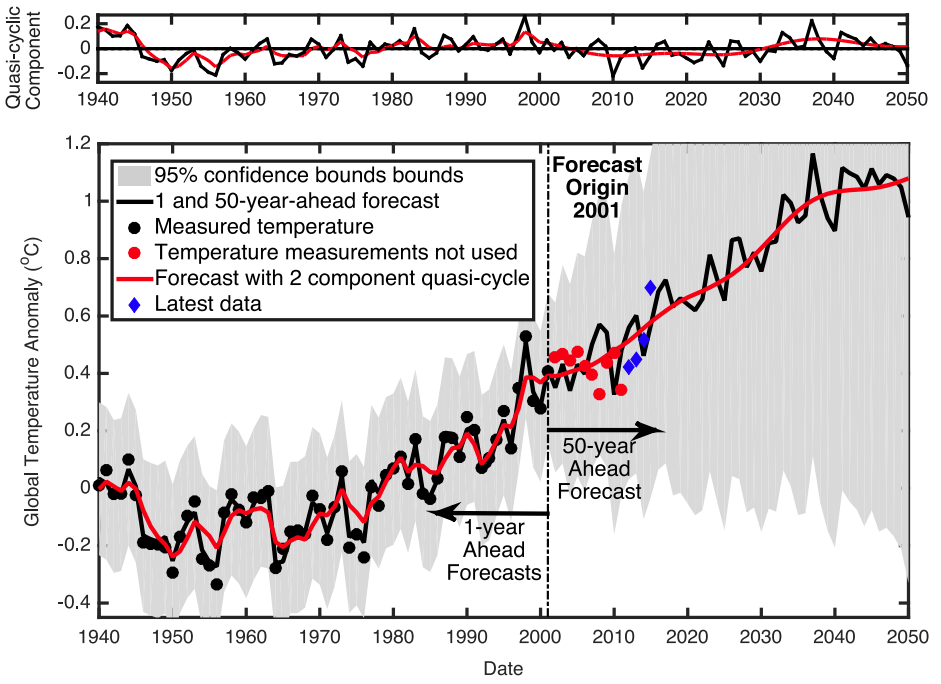

Fig. 7. Final forecasting results obtained using the DBM model: one-year-ahead forecasts up to 2001 and 50-year-ahead thereafter. (For interpretation of the references to colour in this figure legend, the reader is referred to the web version of this article.)

in the present context, it is based solely on the f year ahead forecast output of the continuous-time TF model, where the future input $\hat{u}(k+f|k)$ required for this after 2001 is provided by the DHR forecast of the TRF series discussed in Section 6.1.1.

6.1.4. Final multi-component forecasting

The final multi-component forecast generation is simply the addition of the component forecasts and is shown by the black line in the lower panel of Fig. 7, where the associated 95% confidence bounds take into account the uncertainty arising from all sources, including the large amount of uncertainty emanating from the TRF forecast in Fig. 5. After 2001, we see that it is quite successful in *ex ante* forecasting the actual GTA measurements, shown as red dots, as well as the latest data up to 2015 acquired from the CDIAC web site and shown as blue diamonds. Note that, based on a comparison of these latest data from the web site,[7] where the GTA is now given relative to the 1961–1990 average temperature, with the data used in the present paper, which is based on the GTA relative to 1951–1980 average temperature, this latest series is larger in value by an average of 0.041 °C. In order to ensure consistency, therefore, the plotted points (blue diamonds) have been reduced in value by this same amount. It is clear that the 'levelling' in the forecast temperature rise over the ten year period 2001–2011 is caused by the negative movements in the forecast quasi-cycle discussed in Section 6.1.2 and seen also in the plot of $C(k)$ in the upper panel. This immediately raises the question of whether $C(k)$ is related to other climatic factors and, if so, what these may be. This is considered in Section 7.

The red line in Fig. 7 is the forecast based on using just the first two long period components that dominate the behaviour of the estimated quasi-cycle. This removes the shorter period components, which are less well defined, and so it actually improves the forecasting performance with mean, standard deviation and *Mean Absolute Deviation* (MAD) for the 10-year-ahead forecast from 2001 of 0.0067, 0.071 and 0.057, respectively.

6.2. Rolling forecasts

The HBJ forecasting procedure described in the previous section can be applied anywhere in the series provided the origin of the multi-year forecasts leaves sufficient historical data on which to base the estimation of the model parameters (particularly, in this case, those of the quasi-cyclic model, where a reasonable data length is required to identify the longest period component). At each of these forecast origins, the DBM model parameters are re-estimated and the required forecast of the input forcing $u(k)$ and the quasi-cyclic component $C(k)$ are generated by their updated DHR models, *based only on the data up to the forecast origin and the AIC identified autoregressive spectra computed from these same data*. For instance, if the information in the data up to the forecasting origin suggest a change in the DHR model characteristics and, therefore, in the associated quasi-cycle, then this will be reflected in the forecast.

When this updating procedure is applied in temporal sequence, it produces 'rolling' forecasts that can be useful in various ways. Obviously, such forecasts can confirm

[7] http://cdiac.ornl.gov/ftp/trends/temp/jonescru/global.txt.

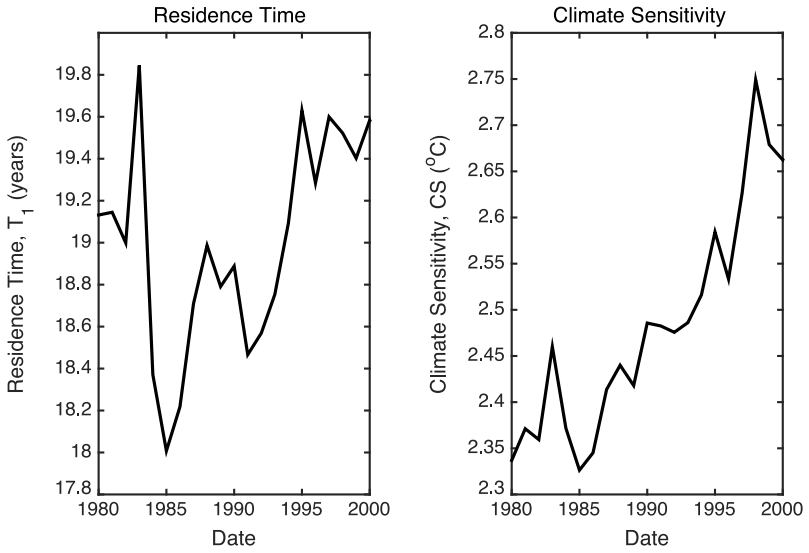

Fig. 8. Changes in the estimated physical parameters of the DBM model, 1980–2000.

that the proposed forecasting engine performs well on a continuing basis over a reasonable period of time (see the set of such rolling forecasts shown in Young, 2014). It can allow also for comparison of this performance with that of other forecasting methods applied in the same manner over the same data. This is discussed in the next Section 6.3.

In addition, since the DBM model is re-estimated on a continuing basis, it is 'adaptive' and so provides information on the changing nature of the estimated model. Fig. 8 is an example of such analysis. It shows the changes in the physically meaningful time constant T_1 and climate sensitivity CS parameters over the period 1980 to 2000. We see that T_1 varies a little in relation to its estimated value in 2001 of 19.31 years but there is no clear movement in any specific direction. In contrast to this, CS rises visibly from 2.34 to around 2.7 compared with the 2001 estimate of 2.59, suggesting that this climatically important parameter *may* be increasing with the passage of time. Of course, these estimates are uncertain and so they must be considered in relation to the estimated 95 percentile uncertainty range based on 1850–2001 data of $\hat{CS} = 2.21 \rightarrow 3.04$ given earlier below Eq. (17).

These results would suggest that, on the basis of the limited data from 1850 to 2001 used in the present analysis, the climate model estimate of CS referred to earlier in Section 3 of 4.3 °C, as well as recent suggestions of even higher sensitivity (Sherwood, Bony, & Dufresne, 2014), appear to be too high. On the other hand, if the upward trend in the adaptive estimates shown in right hand panel of Fig. 8 is significant and continues, then such a higher values might be reached in the future. But this would be entirely speculative when based on such a small set of estimates and any data-based confirmation of such a possibility will have to await the receipt of future data.

6.3. Comparison with other forecasts

There are, of course, numerous methods of modelling and forecasting that could be applied to the GTA data analysed in the previous sub-sections. This section considers the results obtained by two very different methods: the first, based on the well known, fully discrete-time *Box-Jenkins* (BJ) approach that is related to the DBM methodology and represents a standard approach to time series analysis and forecasting that has been used successfully for many years; and one which could not be more different, in which projections of the GTA into the future are generated from the outputs of large, deterministic climate models, such as those discussed previously in Section 3.

6.3.1. Using standard Box-Jenkins (BJ) methodology

The main differences between the standard BJ approach and that used in previous sections are three-fold. First, the TF model is defined in alternative discrete-time, difference equation terms. Second, as mentioned in Section 5.1, a non-stationary input such as the radiative forcing time series $u(k)$ is modelled and forecast using an ARIMA model based on the analysis of the differenced or detrended data. However, the best results in the present example were once again obtained, as in the case of the HBJ continuous-time model estimation, by allowing for initial conditions. Finally, in BJ modelling any seasonality or cyclicity in the data is normally handled using seasonal or periodic differencing which can only be applied if the periodicity is regular and sustained. This is not, therefore, possible in the case on the quasi-cycle component identified in the GTA, so has to be omitted.

The order of the discrete-time TF model in the present example is not particularly well identified (unlike the continuous-time alternative), with several different models producing a reasonable explanation of the data, so there

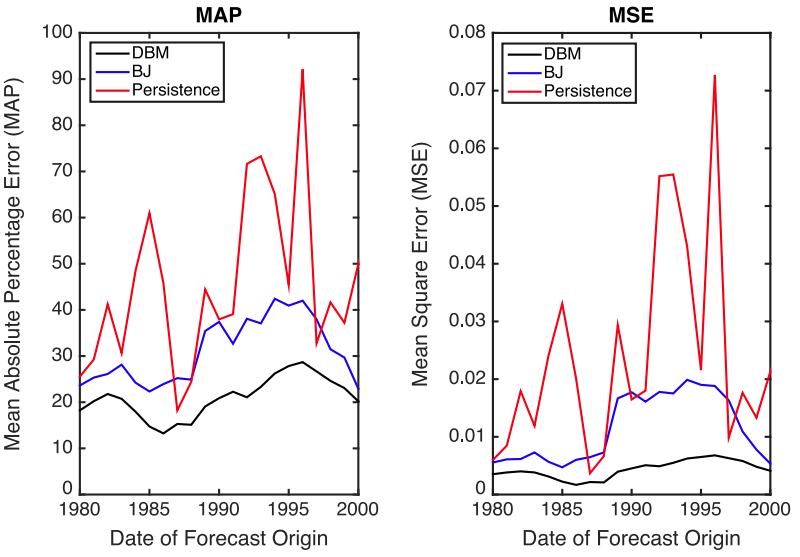

Fig. 9. Relative performance of the DBM, BJ models in terms of the MAP and MSE error measures, with the persistence forecast results shown for reference. (For interpretation of the references to colour in this figure legend, the reader is referred to the web version of this article.)

is no reason to reject the simplest first order model which takes the following form,

$$y(k) = \frac{b_{10}}{1 + a_1 z^{-1}} u(k) + \frac{b_{20}}{1 + a_1 z^{-1}} u_{IC} + \frac{1}{1 + c_1 z^{-1}} e(k) \quad (20)$$

where $u_{IC}(k) = 1.0 \; \forall \; k$, as in the case of the HBJ model (13). The estimates of the main TF model parameters are estimated as follows:

$$\hat{a}_1 = -0.921(0.020); \; \hat{b}_{10} = 0.047(0.008); \\ \hat{c}_1 = 0.569(0.066). \quad (21)$$

This yields a model with $R_T^2 = 0.77$ compared with the $R_T^2 = 0.78$ for the comparable common denominator HBJ model. ARIMA model identification for the input $u(k)$, based on the AIC, suggests a [6 1 0] model and the forecast produced by this is plotted as the black dash-dot line in Fig. 5. As we see, this is quite similar to the forecast produced by the DHR model used for the DBM model forecasting.

Fig. 9 compares the forecasting performance of the above discrete-time BJ model with the equivalent hybrid continuous-time DBM model when they are used to generate rolling, 10-year-ahead GTA forecasts from 1980 to 2000. The main comparative measures used here are the *Mean Absolute Percentage Error* (MAP) and *Mean Square Error* (MSE). Also shown, for reference, are the 'persistence' results, where the forecast for all 10 years is simply the measured value of the GTA at the forecast origin.

When considering the results in Fig. 9, it must be emphasised that, because there is no unique way of performing BJ modelling and forecasting, it is quite possible that other practitioners would produce somewhat different and possibly superior BJ forecasts. Some differences might occur, for example, in the method of modelling the input $u(k)$: e.g. a quadratic trend plus ARIMA model might be used. Or the TF and noise model structures might be identified and estimated differently. Such changes would certainly modify the BJ forecasts shown above. However, if the standard BJ approach is employed, these BJ models would probably not include the quasi-cyclic component. And it is most likely the inclusion of this additional component that creates the main differences in the rolling forecast performance seen in Fig. 9.

6.3.2. Simple DHR modelling and forecasting

Finally, as mentioned in the introduction of the paper, it is important to note that a straightforward and reasonable forecast of the GTA can be obtained simply by applying the DHR model to the GTA time series alone, without any attempt to relate this to the radiative forcing. An example of this is shown in Fig. 10 which was obtained using the dhropt and dhr routines in CAPTAIN to estimate a DHR model that includes an IRW trend and quasi-cycle based, once again, on the AR(29) spectrum of the GTA data. From a simple forecasting standpoint, these results are quite reasonable with the forecast from 2001 predicting the 10 year-ahead 'levelling' behaviour very well, although the subsequent forecast of the latest data points, marked as blue diamonds, is not very good. Indeed, the even simpler forecast, shown as a red line, also does quite well for the first 10 years and is based on a DHR model with only an IRW trend and a stationary (constant frequency, amplitude and phase) sinusoidal cycle of 62 years period. The main limitation of these univariate DHR models, in the present climate modelling context, is that they provide very little insight into the nature of the suggested causal mechanism between the total radiative forcing and the GTA, which is an essential component of the present DBM modelling and forecasting exercise.

6.3.3. Using climate models

Having no personal access to the large climate models used by climate scientists, it has not been possible to generate directly any forecasting results based on these. Moreover, there are a number of such models produced by scientists in different countries (Meehl et al., 2007),

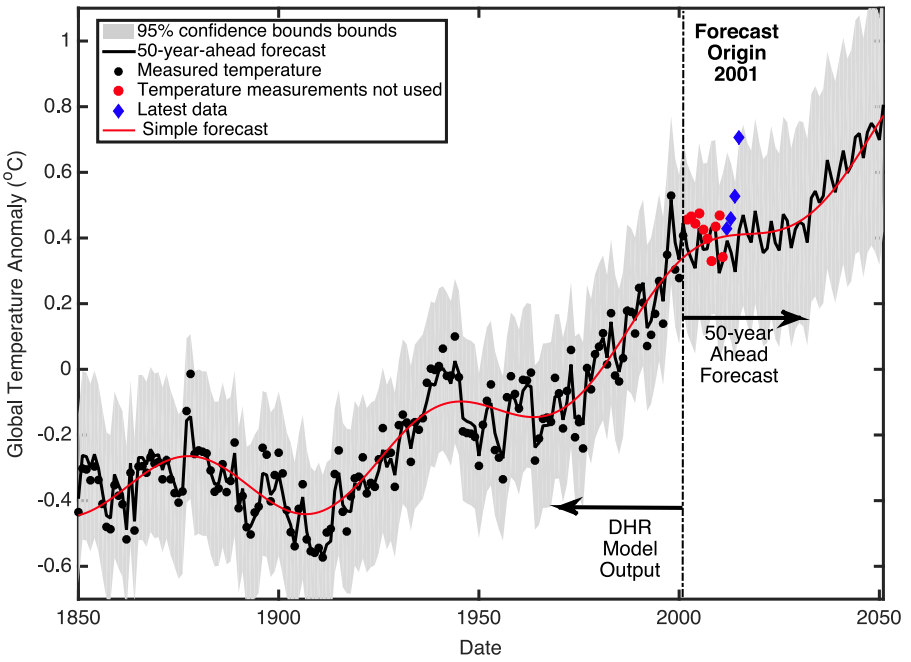

Fig. 10. Forecast of the GTA using the simplest trend plus stationary cycle DHR model. (For interpretation of the references to colour in this figure legend, the reader is referred to the web version of this article.)

so the forecasts they would produce are somewhat different. In addition, climate scientists do not often talk about 'forecasts', as such; rather they refer to 'predictions' or projections' into the future, neither of which are forecasts in the sense used by the present paper. Certainly, their approach is radically different to that employed by either DBM or standard BJ forecasting practitioners.

In this situation, it is necessary to obtain climate model projections from the various data-bases available on the internet. I am very grateful to Professor Geoff Allen in this regard because he has generously passed on information of this kind that he has collected and processed for the period 2000–2010. He informs me that the climate model forecasts were taken from CMIP5 decadal monthly outputs (tas/Amon) with global weighted averages calculated using the reported weights. Outputs were converted from degrees Kelvin to anomalies based on 1961–90 climatology to be consistent with the latest HadCrut4 actual observations. Forecast anomalies were bias corrected based on historical errors for the appropriate step-ahead forecasts, averaged over start dates from 1961 to 1991 at five-year intervals (7 observations). These monthly bias-corrected anomalies in each year are averaged to produce annual forecast anomalies.

I have extracted three examples from Professor Allen's data that relate best to the GTA data that I have used in the previous sub-sections. They are the annual.can1 based on the CanCM4 model with full-field initialization; annual.can2 based on the same model with no initialization of the ocean component; and annual.mpi based on the MPI-ESM-LR model with anomaly initialization. Fig. 11 shows these climate model projections as black, blue and green dots, with the mean of the three plotted as a black line. For the same reason as in Fig. 7, these projections have been reduced by 0.041 °C so that they can be compared with the two DBM model forecasts shown as a red full line and a black dash-dot line representing, respectively, the forecasts using 2 and 13 periodic components in the DHR model of the quasi-cycle.

It is clear that, because of its inclusion of the quasi-cycle, the DBM forecast predicts the levelling after 2000, while the climate projections do not. Also, it is interesting to note that the climate model projections reveal short term fluctuations that are in sympathy with the DBM forecast that uses all 13 periodic components of the DHR model for the quasi-cycle. Unfortunately, however, these fluctuations are in the opposite direction to the short term deviations in the actual GTA data, showing how difficult it is to forecast these short-term phenomena and why it is safer to rely on the forecast that includes only the two smoother, longer term components of the quasi-cycle.

In considering the above results, note that the problem with using the very large climate models for forecasting is not necessarily that they are failing to fully represent the system but rather that their complexity introduces problems of various kinds, such as the difficulties in their optimization and initialization mentioned earlier in Section 1. On the other hand, these are not problems that affect the DBM model very much since both optimization and initialization are handled automatically, making it a much more suitable basis for forecasting the globally averaged data. The fact that the climate model projections do not predict the levelling after 2000 suggests either that other inputs or mechanisms that would create dynamic behaviour such as that seen in the estimated quasi-cycle component of the DBM model are not present, or that they are not being activated in the model simulations. One possibility in this regard is discussed briefly in the next section.

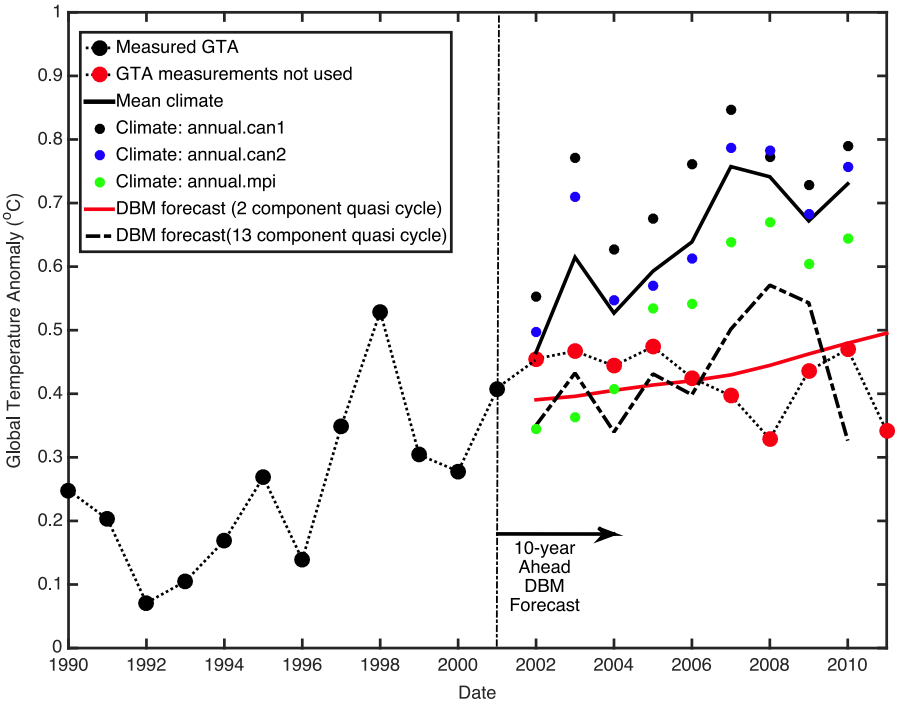

Fig. 11. Comparison of DBM model forecasts and typical climate model projections. (For interpretation of the references to colour in this figure legend, the reader is referred to the web version of this article.)

7. Mechanistic limitations of the DBM Model

The quasi-cyclic component $C(k)$, which is estimated by the time variable parameter DHR model, is difficult to justify in mechanistic terms both because its characteristics change over time and because it reflects the possible presence of a quasi-cycle, the origin of which is not explained. Moreover, its inclusion raises the coefficient of determination R_T^2 from 0.80 to 0.97, so it plays quite a large part in explaining and forecasting the GTA data. It would help to justify the model further, therefore, if an additional input or mechanism in the model could be found that replaces the need for this DHR component. This might also provide clues into a possible mechanistic explanation for the quasi-cyclic behaviour, or at least a reason for further research on this topic.

A number of quasi-cycles have been identified by climate scientists, of which perhaps the best known is the El Niño Southern Oscillation, the cycle of warm and cold temperatures, as measured by the changes of sea surface temperature in the tropical central and eastern Pacific Ocean. AR spectral analysis of the Southern Oscillation Index (SOI) does expose a component with a period of 53 years that exhibits a marginally significant correlation with the quasi cycle identified in the DBM model. However, the one measured climatic phenomenon that I have found to be most promising in this regard is the AMO index series shown in the bottom panel of Fig. 2.

The AMO index is usually defined from the patterns of sea surface temperature variability in the North Atlantic and it is correlated with air temperatures and rainfall over much of the Northern Hemisphere, in particular in the summer climate of North America and Europe. It has been suggested (Schlesinger, 1994) that the quasi-period of the AMO is around 65–70 years but this was based on data up to 1994 and DHR analysis, using series from 1856 to 2001, reveals the quite sharp main peak in the AR(25) spectrum at 60.7 years, with a second peak at 17.6 years. Given the uncertainty in the data and estimation, these are not too far removed from the 48.0 and 19.3 year periods that characterize the most significant peaks in the spectrum of the quasi-cycle identified in Section 5.1 (and other, less significant peaks in the spectrum are also similar). It is important to stress, of course, that we are considering here a quasi-cycle with changing characteristics, so a 'nominal' frequency such as this is not very well defined.

The AMO index, which is also a non-stationary quasi-cycle, is reasonably correlated with the extracted quasi-cyclic component $C(k)$: e.g. the maximum correlation function of 0.47 is well in excess of twice the standard error (2×0.085). Moreover, if a dynamic relationship between these variables is investigated (Young, 2014), a second order TF model is identified between the AMO series and the estimated quasi-cycle $\hat{C}(k)$. This model is much better identified than for the reverse relationship and this direction of causation is supported by Granger causality analysis (e.g. Granger, 1988; Stern & Kaufmann, 2014), using the granger_cause Matlab routine. [8] Consequently, an obvious approach to removing the need for DHR estimation is to consider a stochastic model with two inputs $u(t)$ and the AMO series. This is supported by a few

[8] http://www.mathworks.co.uk/matlabcentral/fileexchange/index?utf8=?&term=granger_cause.

publications in the climate literature (e.g. Mann, Steinman, & Miller, 2014; Meehl, Teng, & Arblaster, 2014), but the most relevant one is the recent paper in 2016 by Chylek, Klett, Dubey, and Hengartner (2016). These authors use *static* linear regression analysis to conclude that "AMO is an effective explanatory variable (predictor) for the 1900–2015 global mean temperature".

When the AMO time series is introduced as a second input into the DBM model and this is then used for forecasting the GTA (Young, 2014), it does not perform quite as well as the DBM model, with an $R_T^2 = 0.965$ compared with $R_T^2 = 0.972$ for the DBM model, mainly because it does not yield quite such good one-year-ahead forecasts. Its main disadvantage in forecasting terms is its relative complexity and robustness. In particular, the simpler DBM forecasting engine does not rely on the second AMO input and it is inherently adaptive because the model parameters are updated at each sampling step. Nevertheless, this reasonably successful exercise in adding the effects of another forcing variable into the DBM transfer function model demonstrates how easy it is to incorporate such additional inputs, as well as adumbrating the potential value of this in such investigative studies.

In this latter regard, DBM modelling can be considered as a potentially useful vehicle for further research on the nature of the dynamic relationships between the globally averaged climate variables; research that could be important also in relation to the development of the large, spatio-temporal climate models, as mentioned in Section 6.3.3. This could include the consideration of other climate variables that may help to explain the quasi-cyclic behaviour or may be influencing both AMO and the quasi-cyclic component of the GTA, $C(k)$; or the possibility of examining whether such relationships can be justified in physical terms as 'tele-connections' (recurring and persistent, large-scale patterns of pressure and circulation anomalies that spans vast geographical areas: see e.g. http://www.cpc.ncep.noaa.gov/data/teledoc/teleintro.shtml and Barnston & Livezey, 1987). For instance, the second order model between AMO and $C(k)$ can be decomposed into a feedback connection of two first order processes (Young, 2014); and Granger causality analysis does not rule out the possibility of an alternative, purely stochastic system, with AMO and $C(k)$ as internal state variables.

The identification and interpretation of the DBM model is reasonably objective. However, it is based on the analysis of data that are affected by any assumptions made by climate scientists in their collection and processing of the data. The analysis of these data is also based, in part, on an acceptance of the existence and direction of the causation between radiative forcing and globally averaged surface temperature assumed by climate scientists. Nevertheless, given the present state of scientific knowledge, both of these assumptions seem scientifically credible and reasonable.

8. Model adaption

It must be emphasised that the analysis reported in previous sections is illustrative rather than exhaustive. For instance, I have not tried to incorporate other potential inputs, such as the SOI series mentioned in Section 7, that may yield improved performance. As new data and information become available, however, these should be utilised to adapt the model parameters, structure and inputs. For instance, the updated forecast from 2011, based entirely on the latest data set (see Section 6.1.4), is shown in Fig. 12. Noting the changes in the series caused by the modified reference level for the anomalies (1961–1990 rather than 1951–1980) and other updates, this is quite similar to the forecast in Fig. 7 and suggests, speculatively of course, another possible levelling episode starting around 2040. Naturally some climatic events, such as volcanic activity, cannot be predicted and any forecasts are subject to errors in this regard, although they should be accommodated within the fairly large uncertainty bounds.

9. Conclusions

This paper has shown that low order, differential equation models are able to both emulate the behaviour of large climate simulation models and form the basis for the identification and estimation of Data-Based Mechanistic (DBM) models that explain quite well the changes in the *Globally-averaged Temperature Anomaly* (GTA) that have been measured over the period 1850 to 2015. In particular, the DBM model identification and estimation procedure identifies a first order differential equation model between the annual measures of *Total Radiative Forcing* (TRF) and the GTA, based on a novel, hybrid (continuous-discrete) form of the well known Box-Jenkins model. It also reveals the presence of a dynamically important, non-stationary quasi-cyclic component of the temperature response that can be modelled well by a *Dynamic Harmonic Regression* (DHR) model. The complete unobserved component model, combining these two components, yields quite good short-to-medium term forecasts of global temperature changes, including a prediction, based only on the data up to 2001, of the levelling in temperature rises that occurred between the start of the new Millennium and 2014. The model also suggests that, *on the basis of the limited 1850–2001 data used here*, the climate sensitivity suggested by the large climate models of over 4 °C may be be somewhat too high, when compared with the 5 $\leftrightarrow$ 95 percentile uncertainty range of 2.21 $\rightarrow$ 3.03 °C estimated here, even allowing for the estimation uncertainty and a possible trend in the estimated values over the period 1980–2001.

The paper also notes that the estimated quasi-cyclic component is quite well correlated with the *Atlantic Multi-decadal Oscillation* (AMO) index and points out how this has been incorporated successfully as a second input into the DBM model so removing, to quite a large extent, the need for the stochastic quasi-cyclic component in the model. Whilst the specific use of the AMO as an input is speculative, it suggests the need for more research on the physical nature and causes of these quasi-cyclic variations in the GTA. In this same regard, the paper has shown that some typical examples of climate model forecasts made over the post-Millenium period are not able to capture the levelling effect in the GTA. It would seem, therefore, that they might also benefit from more research on the origin of the quasi-cyclic changes in the GTA and the incorporation or activation of mechanisms that introduce this behaviour into the model projections.

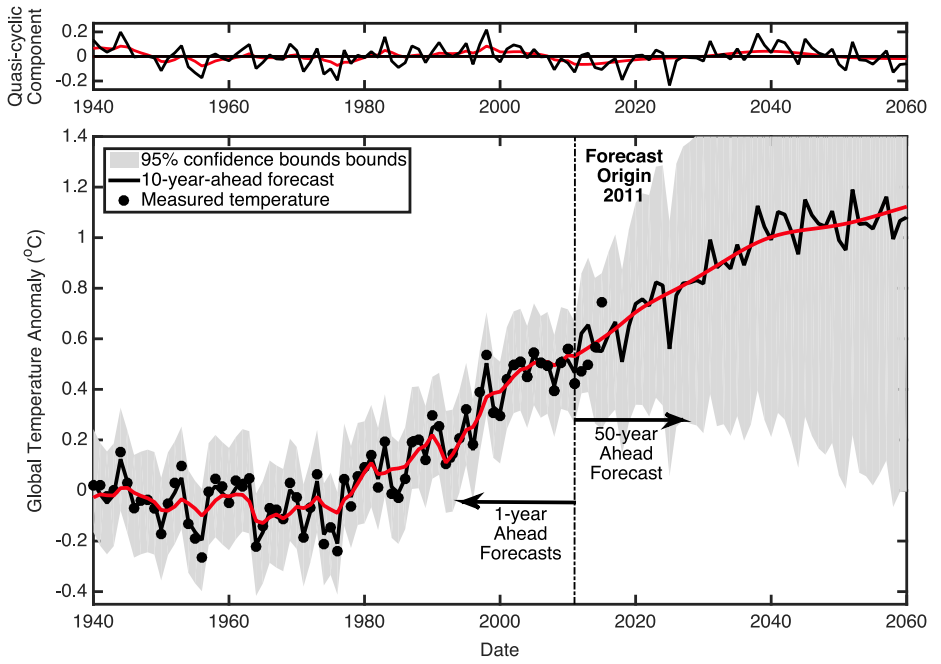

Fig. 12. 50 year forecast from 2011 using the updated DBM model based on the latest data from 1850 to 2011.

Particularly when it is considered from a DBM standpoint, climate system modelling has to be an on-going, adaptive process. For this reason, it is important to stress that the DBM model developed in this paper represents just one attempt at the identification of a causative stochastic, dynamic model that can be interpreted in mechanistic terms and provides, at this point in time, a reasonable basis for short-term forecasting and control. But the whole essence of DBM modelling is to extract as much information as possible from the data and so, as new data and information become available, these should be utilised to adapt the model parameters and, if necessary, the model structure and input variables.

Finally, it is important to note that the DBM model identified in this paper is not limited to ex-ante forecasting. It can also function as a stochastic simulation model that can be used for 'what-if' exercises relating, for example, to different human activities such as emissions control and management. Moreover, because it is a model that is well suited to the application of optimal control system design techniques, it is able to evaluate emissions strategies that exploit control system design in order to provide, for example, year-by-year emissions advice. This advice could relate to the emissions required to achieve some desired changes of variables such as the globally averaged levels of surface temperature, carbon dioxide, and sea level (e.g. DBM models of CO_2 and sea level have been identified for such studies); or the optimization of some specified criterion function that could include both technical and socio-economic considerations. Some initial, simple exercises of this kind, using the DBM model identified in this paper, are described in a recent technical report (Young, 2017) [9].

[9] This will be made available from http://captaintoolbox.co.uk/Captain_Toolbox.html/Publication_Downloads.html.

Acknowledgments

This paper has been influenced by discussions with Professor Antonio Garcia-Ferrer and has benefited by support from the project Programa Estatal de Investigacion 2013-2016, Spain (ECO2015-70331-C2-1-R). I am very grateful to a number of other people who have helped me with the paper. Dr. David Leedal supplied the Matlab version of the MAGICC model and associated advice; Professor Geoff Allen generously provided the climate model data and outputs used in Fig. 11 and also useful comments on the paper; Professor Robert Fildes urged me to write the paper and also provided useful comments; and Dr. Granville Tunnicliffe-Wilson provided information on standard Box-Jenkins analysis. I also thank two anonymous reviewers who made very useful comments; and various climate science sources who provided free access to the data used in my analysis. Of course, I remain responsible for any errors and omissions in the paper.

References

Akaike, H. (1974). A new look at statistical model identification. *IEEE Transactions on Automatic Control*, *19*, 716–723.

Barnston, A. G., & Livezey, R. E. (1987). Classification, seasonality and persistence of low-frequency atmospheric circulation patterns. *Monthly Weather Review*, *115*, 1083–1126.

Box, G. E. P., & Jenkins, G. M. (1970). *Time series analysis forecasting and control*. San Francisco: Holden-Day.

Box, G. E. P., Jenkins, G. M., & Reinsel, G. C. (1994). *Time series analysis: forecasting and control*. (3rd ed.). Upper Saddle River, NJ, USA: Prentice Hall PTR.

Chylek, P., Klett, J., Dubey, M., & Hengartner, N. (2016). The role of atlantic multidecadal oscillation in the global mean temperature variability. *Climate Dynamics*, *47*, 3271–3279.

Cubasch, U., et al. (2001). Projections of future climate change. In J. T. Houghton, et al. (Eds.), *Climate change 2001: the scientific basis* (pp. 525–582). New York: Cambridge University Press.

Fildes, R., & Kourentzes, N. (2011). Validation and forecasting accuracy in models of climate change. *International Journal of Forecasting*, *27*(4), 968–995.

Garnier, H., & Young, P. C. (2014). The advantages of directly identifying continuous-time transfer function models in practical applications. *International Journal of Control*, *87*(7), 1319–1338.

Geoffroy, O., Saint-Martin, D., Olivié, D. J. L., Voldoire, A., Bellon, G., & Tytéca, S. (2013). Transient climate response in a two-layer energy-balance model. part I: Analytical solution and parameter calibration using CMIP5 AOGCM experiments. *Journal of Climate*, *26*, 1841–1857.

Granger, C. W. (1988). Some recent developments in a concept of causality. *Journal of Econometrics*, *39*, 199–211.

Harvey, A. C. (1989). *Forecasting structural time series models and the kalman filter*. Cambridge: Cambridge University Press.

Hasselmann, K., Hasselmann, S., Giering, R., Ocana, V., & Storch, H. V. (1997). Sensitivity study of optimal co_2 emission paths using a simplified structural integrated assessment model (SIAM). *Climate Change*, *37*, 345–386.

Hasselmann, K., Sausen, R., Maier-Reimer, E., & Voss, R. (1993). On the cold start problem in transient simulations with coupled atmosphere-ocean models. *Climate Dynamics*, *9*, 53–61.

Hooss, G., Voss, R., Hasselman, K., Maier-Reimer, E., et al. (2001). A nonlinear impulse response model of the coupled carbon cycle-climate system (NICCS). *Climate Dynamics*, *18*, 189–202.

Jarvis, A. J., Leedal, D. T., Taylor, C. J., & Young, P. C. (2009). Stabilizing global mean surface temperature: A feedback control perspective. *Environmental Modelling & Software*, *24*, 665–674.

Jarvis, A. J., & Li, S. (2011). On the timescale-gain relationship of climate models. *Climate Dynamics*, *36*, 523–531.

Jarvis, A. J., Young, P. C., Leedal, D. T., & Chotai, A. (2008). A robust sequential CO_2 emissions strategy based on optimal control of atmospheric CO_2 concentrations. *Climate Change*, *86*, 357–373.

Kaufmann, R. K., Kauppi, H., & Stock, J. H. (2006a). Emissions, concentrations and temperature: a time series analysis. *Climate Change*, *77*, 249–278.

Kaufmann, R. K., Kauppi, H., & Stock, J. H. (2006b). The relationship between radiative forcing and temperature: what do statistical analyses of the instrumental temperature record measure? *Climate Change*, *77*, 279–289.

Knutti, R., & Hegerl, G. C. (2008). The equilibrium sensitivity of the earth's temperature to radiation changes. *Nature Geoscience*, *1*(11), 735–743.

Li, S., & Jarvis, A. J. (2009). Long run surface temperature dynamics of an AOGCM: the HadCM3 49CO2 forcing experiment revisited. *Climate Dynamics*, *33*, 817–825.

Li, S., Jarvis, A., & Leedal, D. T. (2009). Are response function representations of the global carbon cycle ever interpretable? *Tellus B*, *61*(2), 361–371.

Lowe, J. (2003). Parameters for tuning a simple climate model. URL http://unfccc.int/resource/brazil/climate.html.

Mann, M. E., Steinman, B. A., & Miller, S. K. (2014). On forced temperature changes, internal variability, and the AMO. *Geophysical Research Letters*, *41*, 3211–3219.

Meehl, G. A., Covey, C., Taylor, K. E., Delworth, T., Stouffer, R. J., Latif, M., et al. (2007). The WCRP CMIP3 multimodel dataset: A new era in climate change research. *Bulletin of the American Meteorological Society*, *88*(9), 1383–1394.

Meehl, G. A., Teng, H., & Arblaster, J. M. (2014). Climate model simulations of the observed early-2000s hiatus of global warming. *Nature Climate Change*, *4*, 898–902.

Meinshausen, M., Raper, S. C. B., & Wigley, T. M. L. (2011). Emulating coupled atmosphere-ocean and carbon cycle models with a simpler model, MAGICC6 –Part 1: Model description and calibration. *Atmospheric Chemistry and Physics Discussions*, *11*, 417–1456.

Mills, T. C. (2009). How robust is the long-run relationship between temperature and radiative forcing?. *Climatic Change*, *94*, 351–361.

Mills, T. (2010). 'skinning a cat': alternative models of representing temperature trends. *Climatic Change*, *101*(3–4), 415–426.

Myhre, G., Highwood, E. J., Shine, K. P., & Stordal, F. (1998). New estimates of radiative forcing due to well mixed greenhouse gases. *Geophysical Research Letters*, *25*, 2715–2718.

Neelin, J. D., Bracco, A., Luo, H., McWilliams, J. C., & Meyerson, J. E. (2010). Considerations for parameter optimization and sensitivity in climate models. *Proceedings of the National Academy of Sciences*, *107*(50), 21349–21354.

Pedregal, D. J., & Young, P. C. (2002). Statistical approaches to modelling and forecasting time series. In M. P. Clements, & D. F. Hendry (Eds.), *A companion to economic forecasting* (pp. 69–104). Oxford: Blackwell.

Popper, K. (1959). *The logic of scientific discovery*. London: Hutchinson.

Priestley, M. B. (1981). *Spectral analysis and time series*. London: Academic Press.

Schlesinger, M. E. (1994). An oscillation in the global climate system of period 65-70 years. *Nature*, *367*(6465), 723–726.

Shackley, S., Young, P. C., Parkinson, S., & Wynne, B. (1998). Uncertainty, complexity and concepts of good science in climate change modelling: are GCMs the best tools? *Climatic Change*, *38*, 159–205.

Sherwood, S. C., Bony, S., & Dufresne, J.-L. (2014). Spread in model climate sensitivity traced to atmospheric convective mixing. *Nature*, *505*(7481), 37–42. URL http://dx.doi.org/10.1038/nature12829.

Stern, D. I., & Kaufmann, R. (2014). Anthropogenic and natural causes of climate change. *Climatic Change*, *122*, 257–269.

Stouffer, R. J., & Manabe, S. (1994). Multiple-century response of a coupled ocean- atmosphere model to an increase of atmospheric carbon dioxide. *Journal of Climate*, *7*, 5–23.

van Hateren, J. H. (2013). A fractal climate response function can simulate global average temperature trends of the modern era and the past millennium. *Climate Dynamics*, *40*(11), 2651–2670.

Young, P. C. (1979). Self-adaptive Kalman filter. *Electronics Letters*, *15*(12), 358–360.

Young, P. C. (1999). Data-based mechanistic modelling, generalised sensitivity and dominant mode analysis. *Computer Physics Communications*, *117*, 113–129.

Young, P. C. (2000). Stochastic,dynamic modelling and signal processing: time variable and state dependent parameter estimation. In W. J. Fitzgerald, A. Walden, R. Smith, & P. C. Young (Eds.), *Nonlinear and nonstationary signal processing* (pp. 74–114). Cambridge: Cambridge University Press.

Young, P. C. (2006). The data-based mechanistic approach to the modelling, forecasting and control of environmental systems. *Annual Reviews in Control*, *30*, 169–182.

Young, P. C. (2010). Gauss, Kalman and advances in recursive parameter estimation. *Journal of Forecasting*, *30*, 104–146 (Special Issue Celebrating 50 Years of the Kalman Filter).

Young, P. C. (2011). *Recursive estimation and time-series analysis: an introduction for the student and practitioner*. Berlin: Springer-Verlag.

Young, P. C. (2012). Data-based mechanistic modelling: natural philosophy revisited? In L. Wang, & H. Garnier (Eds.), *System identification, environmetric modelling and control* (pp. 321–340). London: Springer-Verlag.

Young, P. C. (2013). Hypothetico-inductive data-based mechanistic modeling of hydrological systems. *Water Resources Research*, *49*(2), 915–935.

Young, P. C. (2014). Hypothetico-inductive data-based mechanistic modelling, forecasting and control of global temperature, Tech. rep. Lancaster Environment Centre, Lancaster University, UK.

Young, P. C. (2015). Refined instrumental variable estimation: Maximum likelihood optimization of a unified Box-Jenkins model. *Automatica*, *52*, 35–46.

Young, P. C. (2017). Emission control strategies to achieve desirable global climate outcomes using Data Based Mechanistic (DBM) models and control system design: some initial thoughts, Tech. rep. Lancaster Environment Centre.

Young, P. C., & Jakeman, A. J. (1979). Refined instrumental variable methods of time-series analysis: Parts I, II and III. *International Journal of Control*, *29*, 1–30 29 (1979), 621–644; (1980) 31, 741–764.

Young, P. C., & Jarvis, A. J. (2002). Data-based mechanistic modelling, the global carbon cycle and global warming, Tech. rep. Lancaster Environment Centre, Lancaster University, UK.

Young, P. C., & Parkinson, S. (2002). Simplicity out of complexity. In M. B. Beck (Ed.), *Environmental foresight and models: A manifesto* (pp. 251–294). Oxford: Elsevier.

Young, P. C., Parkinson, S., & Lees, M. J. (1996). Simplicity out of complexity: Occam's razor revisited. *Journal of Applied Statistics*, *23*, 165–210.

Young, P. C., & Pedregal, D. J. (1999). Recursive and en-bloc approaches to signal extraction. *Journal of Applied Statistics*, *26*, 103–128.
Young, P. C., Pedregal, D. J., & Tych, W. (1999). Dynamic harmonic regression. *Journal of Forecasting*, *18*, 369–394.
Young, P. C., & Ratto, M. (2009). A unified approach to environmental systems modeling. *Stochastic Environmental Research and Risk Assessment*, *23*, 1037–1057.
Young, P. C., & Ratto, M. (2011). Statistical emulation of large linear dynamic models. *Technometrics*, *53*, 29–43.

Peter C. Young is Emeritus Professor of Environmental Systems at Lancaster University and Adjunct Professor in the Fenner School of Environment and Society at the Australian National University, Canberra. Before taking up his position as as Head of the Environmental Science Department at Lancaster in 1981, he was a Lecturer in Engineering and Fellow of Clare Hall Cambridge (1970–1975) and Professorial Fellow at the Australian National University (1975–1981). In 1987, he was instrumental in establishing the Institute of Environmental and Biological Sciences at Lancaster. He helped to set up the Lancaster Centre for Forecasting with Prof. Robert Fildes in 1992 and directed the Centre for Research on Environmental Systems and Statistics until his retirement. He has published over 300 papers and chapters in books, as well as writing and editing several books, including latterly: *Recursive Estimation and Time Series Analysis* (2011) and *True Digital Control* (2013), the latter co-authored with James Taylor and Arun Chotai. He continues to pursue research on model identification and estimation, as well as data-based mechanistic modelling, forecasting and control, with applications in various areas of research and development.